NAVAL POSTGRADUATE SCHOOL

MONTEREY, CALIFORNIA

THESIS

PERFORMANCE ANALYSIS OF 802.16A

by

Jared L. Allen

June 2005

Thesis Advisor: Tri T. Ha
Second Reader: David Jenn

Approved for public release; distribution is unlimited

THIS PAGE INTENTIONALLY LEFT BLANK

REPORT DOCUMENTATION PAGE			Form Approved OMB No. 0704–0188
Public reporting burden for this collection of information is estimated to average 1 hour per response, including the time for reviewing instruction, searching existing data sources, gathering and maintaining the data needed, and completing and reviewing the collection of information. Send comments regarding this burden estimate or any other aspect of this collection of information, including suggestions for reducing this burden, to Washington headquarters Services, Directorate for Information Operations and Reports, 1215 Jefferson Davis Highway, Suite 1204, Arlington, VA 22202–4302, and to the Office of Management and Budget, Paperwork Reduction Project (0704–0188) Washington DC 20503.			
1. AGENCY USE ONLY ***(Leave blank)***	**2. REPORT DATE** June 2005	**3. REPORT TYPE AND DATES COVERED** Master's Thesis	
4. TITLE AND SUBTITLE: Performance Analysis of 802.16a			**5. FUNDING NUMBERS**
6. AUTHOR(S) Jared Allen			
7. PERFORMING ORGANIZATION NAME(S) AND ADDRESS(ES) Naval Postgraduate School Monterey, CA 93943–5000			**8. PERFORMING ORGANIZATION REPORT NUMBER**
9. SPONSORING /MONITORING AGENCY NAME(S) AND ADDRESS(ES) N/A			**10. SPONSORING/MONITORING AGENCY REPORT NUMBER**
11. SUPPLEMENTARY NOTES The views expressed in this thesis are those of the author and do not reflect the official policy or position of the Department of Defense or the U.S. Government.			
12a. DISTRIBUTION / AVAILABILITY STATEMENT Approved for public release; distribution is unlimited.			**12b. DISTRIBUTION CODE**

13. ABSTRACT (maximum 200 words)

With the ever–increasing popularity of wireless internet, its scale is broadening. While the IEEE 802.15 standard provides the parameters necessary for a wireless personal area network (WPAN), the IEEE 802.16a standard provides broadband wireless access (BWA), or a wireless metropolitan area network (WMAN). Popularly referred to as Wi–Max, the standard uses cellular topography with a base station and subscriber station and cuts down on infrastructure and thus can be used in most environments. The 802.16a standard can take advantage of the popular OFDM modulation technique. This thesis takes a developed synchronization algorithm and tests its performance on 802.16a. In addition, it tests the standard's performance in different types of channel. Various techniques are evaluated including interleaving and antenna diversity. The 802.16a standard employs a form of transmit diversity called Space–Time Coding. The transmit diversity is compared with Maximal–Ratio Combining receiver diversity. The evaluation was done in simulation developed in Matlab; the simulations show drastic improvement when using the aforementioned techniques, particularly diversity.

14. SUBJECT TERMS 802.16a, BWA, WMAN, Wi–MAX, OFDM, Packet Detection, Frequency Synchronization, Frame Synchronization, Channel Estimation, Carrier Offset, Phase Noise, Pilot Phase Tracking, Equalizaton, Randomizing, Convolutional Code, Reed–Solomon Code, Reed–Solomon Concatenated Code, Interleaving, Puncturing, Diversity, Space–Time Coding, Viterbi Algorithm, Soft–Decision Decoding			**15. NUMBER OF PAGES** 95
			16. PRICE CODE
17. SECURITY CLASSIFICATION OF REPORT Unclassified	**18. SECURITY CLASSIFICATION OF THIS PAGE** Unclassified	**19. SECURITY CLASSIFICATION OF ABSTRACT** Unclassified	**20. LIMITATION OF ABSTRACT** UL

NSN 7540–01–280–5500

Standard Form 298 (Rev. 2–89)
Prescribed by ANSI Std. 239–18

THIS PAGE INTENTIONALLY LEFT BLANK

Approved for public release; distribution is unlimited

PERFORMANCE ANALYSIS OF 802.16A

Jared L Allen
Ensign, United States Navy
B.S., United States Naval Academy, 2004

Submitted in partial fulfillment of the
requirements for the degree of

MASTER OF SCIENCE IN ELECTRICAL ENGINEERING

from the

NAVAL POSTGRADUATE SCHOOL
June 2005

Author: Jared L Allen

Approved by: Tri T. Ha
Thesis Advisor

David Jenn
Second Reader

John P. Powers
Chairman, Department of Electrical and Computer Engineering

THIS PAGE INTENTIONALLY LEFT BLANK

ABSTRACT

With the ever–increasing popularity of wireless internet, its scale is broadening. While the IEEE 802.15 standard provides the parameters necessary for a wireless personal area network (WPAN), the IEEE 802.16a standard provides broadband wireless access (BWA) or a wireless metropolitan area network (WMAN). Popularly referred to as Wi–Max, the standard uses cellular topography with a base station and subscriber station and cuts down on infrastructure and thus can be used in most environments. The 802.16a standard can take advantage of the popular OFDM modulation technique. This thesis takes a developed synchronization algorithm and tests its performance on 802.16a. In addition, it tests the standard's performance in different types of channel. Various techniques are evaluated including interleaving and antenna diversity. The 802.16a standard employs a form of transmit diversity called Space–Time Coding. The transmit diversity is compared with Maximal–Ratio Combining receiver diversity. The evaluation was done in simulation developed in Matlab; the simulations show drastic improvement when using the aforementioned techniques, particularly diversity.

THIS PAGE INTENTIONALLY LEFT BLANK

TABLE OF CONTENTS

I. INTRODUCTION....1
A. OBJECTIVE....2
B. THESIS OUTLINE....3

II. BACKGROUND....5
A. CHANNEL MODEL....5
1. Multipath Fading....6
a. Large–Scale Propagation Loss....7
b. Small–Scale Fading....7
c. Rayleigh Fading Model....9
B. 802.16A OVERVIEW....10
1. 802.16 Architecture....10
2. MAC Layer....12
3. 802.16a PHY Overview....13
a. WirelessMAN – SCa....13
b. WirelessMAN – OFDM....16
c. WirelessMAN – OFDMA....18
C. SUMMARY....20

III. SYNCHRONIZATION....21
A. THE 802.16A PREAMBLE....21
B. PACKET DETECTION....24
1. Packet Detection with Preamble....25
2. Packet Detection without Preamble....26
C. TIME SYNCHRONIZATION....27
D. FREQUENCY SYNCHRONIZATION....27
1. Maximum Likelihood (ML) Estimation of Frequency Offset....29
2. Properties of the ML Estimation Algorithm....30
E. COMBINED TIME AND FREQUENCY SYNCHRONIZATION....32
F. CARRIER PHASE TRACKING....37
G. CHANNEL ESTIMATION....39
1. Frequency Domain Method....39
2. Time-Domain Method....40
H. EQUALIZATION....41
I. SUMMARY....41

IV. PERFORMANCE OF 802.16A....43
A. OVERVIEW OF 802.16A FRAME AND TRANSMISSION PROCESS....43
B. TRANSMITTER....44
C. RECEIVER....50
D. PERFORMANCE OF 802.16A IN AWGN....52
E. PERFORMANCE OF 802.16A IN MULTIPATH FADING....58

F. SPACE–TIME CODING DIVERSITY 63
G. SUMMARY 66
V. CONCLUSIONS AND FUTURE WORK 69
A. CONCLUSIONS 69
B. FUTURE WORK 70
LIST OF REFERENCES 71
INITIAL DISTRIBUTION LIST 73

LIST OF FIGURES

Figure 1. Example of FDD (From Ref. [1].) 11
Figure 2. Example of TDD (From Ref. [1].) 12
Figure 3. IEEE 802.16 Protocol Structure showing SAP's (From Ref. [1].) 13
Figure 4. SCa Burst Frame (From Ref. [1].) 14
Figure 5. TCM Coder for Rate 3/4 16–QAM (From Ref. [1].) 15
Figure 6. TCM Constellation for 16–QAM (From Ref. [1].) 15
Figure 7. Paired Blocks for STC Transmit Diversity Combining (From Ref. [1].) 16
Figure 8. OFDMA Frequency Domain and Subchannels (From Ref. [1].) 18
Figure 9. Sample OFDMA TDD Frame (From Ref. [1].) 19
Figure 10. Short Preamble (From Ref [1].) 22
Figure 11. Long Preamble (From Ref [1].) 23
Figure 12. Sequence of 128 Samples (Real Part) 23
Figure 13. Sequence of 64 Samples (Real Part) 24
Figure 14. Block Diagram of Delay and Correlate Algorithm (From Ref. [4].) 25
Figure 15. Packet Detection with Preamble (SNR = 0 dB) 26
Figure 16. DFT Window Timing (From Ref. [4].) 27
Figure 17. Overlapping Orthogonal Carriers (From Ref. [4].) 28
Figure 18. Flow Chart of the Combined Synchronization Algorithm (From Ref. [4].) 33
Figure 19. Decision Statistic m_n in AWGN Channel with SNR = 10 dB and D = 192 34
Figure 20. PDF of Symbol Timing Estimate in AWGN, SNR = 10 dB 35
Figure 21. PDF of Frequency Offset Estimate in AWGN, SNR = 10 dB 35
Figure 22. PDF of Symbol Timing Estimate in Rayleigh Fading Channel with RMS Delay Spread = 400 ns, SNR = 10 dB 36
Figure 23. PDF of Frequency Offset Estimate in Rayleigh Fading Channel with RMS Delay Spread = 400 ns, SNR = 10 dB 36
Figure 24. QPSK Constellation Rotation with 3-kHz Frequency Error 38
Figure 25. OFDM TDD Frame (From Ref. [1].) 43
Figure 26. 802.16a PHY Transmitter (From Ref. [1].) 45
Figure 27. Bit Randomizer (From Ref. [1].) 45
Figure 28. Binary rate 1/2 Convolutional Encoder (From Ref. [1].) 46
Figure 29. Bit Error Rate of IEEE 802.16a rate 1/2 QPSK with and without Interleaving in 200–ns RMS Delay Spread Rayleigh Fading Channel 48
Figure 30. Gray Mapped 16–QAM (From Ref. [1].) 48
Figure 31. Pilot Symbol Generator (From Ref. [1].) 49
Figure 32. Transmitted Signal in the Time Domain 50
Figure 33. Signal with 20-MHz Bandwidth with Spectral Mask 50
Figure 34. Rate 1/2 16–QAM Constellation in AWGN (SNR = 18 dB) 52
Figure 35. BER of Rate 3/4 64–QAM in AWGN 53
Figure 36. PER of Rate 3/4 64–QAM 54
Figure 37. BER of Rate 2/3 64–QAM 55
Figure 38. PER of Rate 2/3 64–QAM 55

Figure 39. 802.16a BER in AWGN 56
Figure 40. 802.16a PER in AWGN....57
Figure 41. Signal Constellation in 50-ns RMS Delay Spread Rayleigh Fading Channel with SNR = 20 dB 59
Figure 42. Equalized 16–QAM Signal in 50-ns RMS Delay Spread with SNR = 20 dB....59
Figure 43. Rate 3/4 QPSK in RMS = 500 ns Delay Spread....60
Figure 44. QPSK in a Rayleigh Fading Channel with RMS Delay Spread of 200 ns 61
Figure 45. 16–QAM in 200-ns RMS Delay Spread Rayleigh-Fading Channel....62
Figure 46. 64–QAM in RMS = 200 ns Rayleigh Fading Channel....63
Figure 47. Block Diagram of STC Encoding and Decoding (From Ref. [1].)....64
Figure 48. Rate 3/4 64–QAM using Maximal–Ratio Combining Receiver Diversity and STC Transmit Diversity....66

LIST OF TABLES

Table 1. Types of Small–Scale Fading (After Ref. [3].) 6
Table 2. STC Transmission for SCa (From Ref. [1].) 16
Table 3. OFDM Symbol Parameters (From Ref. [1].) 17
Table 4. OFMA DL Carrier Allocations (From Ref. [1].) 19
Table 5. OFDM Supported Punctured Code Rates (From Ref. [1].) 46
Table 6. Mandatory Channel Coding per Modulation (From Ref. [1].) 47
Table 7. Normalized Power Constants (From Ref. [1].) 49
Table 8. Space–Time Coding 64
Table 9. MIMO STC 65

THIS PAGE INTENTIONALLY LEFT BLANK

ACKNOWLEDGMENTS

First, I would like to thank my friends and family for supporting me during my time here. Their encouragement helped me enjoy my time here.

I would also like to thank my thesis advisor Dr. Ha for his assistance and support as well as Nathan Beltz for providing the necessary equipment for my thesis.

THIS PAGE INTENTIONALLY LEFT BLANK

LIST OF ACRONYMS AND/OR ABBREVIATIONS

AAS	Adaptive Antennas System
AWGN	Additive White Gaussian Noise
BER	Bit Error Rate
BS	Base Station
BTC	Block Turbo Coding
BWA	Broadband Wireless Access
CIR	Channel Impulse Response
CP	Cyclic Prefix
CTC	Convolutional Turbo Coding
DFT	Discrete Fourier Transform
DL	Downlink
DSL	Digital Subscriber Line
FCH	Frame Control Header
FDD	Frequency Division Duplexing
FEC	Forward Error Correction
FFT	Fast Fourier Transform
GUI	Graphical User Interface
HDD	Hard Decision decoding/Demodulation
ICI	Inter-Carrier Interference
IEEE	Institute of Electrical and Electronic Engineers
ISI	Inter-Symbol Interference

LAN	Local Area Network
LOS	Line of Sight
MAC	Medium Access Control
MIMO	Multiple Input Multiple Output
MISO	Multiple Input Single Output
ML	Maximum Likelihood
MP-MP	Multipoint-to-Multipoint
MRC	Maximal-Ratio Combining
OFDM	Orthogonal Frequency Division Multiplexing
OFDMA	Orthogonal Frequency Division Multiple Access
PDF	Probability Density Function
PER	Packet Error Rate
PMP	Point-to-Multipoint
PHY	Physical Layer
QoS	Quality of Service
QPSK	Quadrature Phase Shift Keying
RS	Reed-Solomon Code
SAP	Service Access Point
SCa	802.16a – Single Carrier
SDD	Soft Decision Decoding/Demodulation
SNR	Signal-to-Noise Ratio
SS	Subscriber Station
STC	Space-Time Coding
TDD	Time Division Duplexing

UL	Uplink
WLAN	Wireless Local Area Network
WMAN	Wireless Metropolitan Area Network

THIS PAGE INTENTIONALLY LEFT BLANK

EXECUTIVE SUMMARY

Broadband internet access demand is always increasing. As a result, it is reaching places that until recently could not get internet. Currently, infrastructure constraints limit digital subscriber lines (DSL) and cable availability particularly in more sparsely populated environments. The IEEE 802.16a standard provides broadband wireless access (BWA) in the 2-11 GHz band of the spectrum. This frequency range allows for non-line of sight (non-LOS) communication, since multipath still contributes a substantial amount of received signal energy. The standard incorporates several newly developed technologies to attain its high data rates. Three modes of modulation are available to any 802.16a standard. They are single carrier, orthogonal frequency division multiplexing (OFDM), and orthogonal frequency division multiple access (OFDMA). The 802.16a standard could also be used on the battlefield to provide higher bandwidth services for more functionality. Since 802.16a uses orthogonal frequency division multiplexing (OFDM), subcarriers that receive intentional interference can be modulated with "dummy" symbols in order for the system to continue functioning without modification at the receiver. This thesis analyzed the performance of the standard in different environments using a simulation developed in Matlab.

OFDM allows for the wireless transmission of broadband signals. OFDM is an area of current study and is employed on several recently developed technologies like 802.11. OFDM uses multiple orthogonal subcarriers overlapped in order to create a spectrally efficient manner of transmitting bits in parallel. OFDM also is more resistant to frequency fading since the bandwidth of the individual subcarriers is much less than that of the overall signal.

Multipath and fading can lead to signal distortion and inter-symbol interference (ISI). OFDM systems including 802.16a make use of a cyclic prefix (CP) that allows for time after each OFDM symbol to collect the multipath signals without interference with the following symbol. Inter-carrier interference can be avoided by making the CP an extension of the end of the symbol.

Since the OFDM subcarriers are so tightly overlapped, synchronization in both the frequency and time domains is of high importance. Any frequency offset can cause a loss of orthonogality at the receiver leading to significant amounts ICI, while a time offset can cause an improper decision of the beginning of the OFDM symbol leading to ISI. Therefore, the receiver must be able to synchronize the signal to a much finer degree than in single-carrier systems. The 802.16a standard must also be able to estimate the channel, done by using a preamble, or sequence of known symbols. Channel estimation allows for coherent detection, equalization, and diversity. This thesis modified and tested an already developed synchronization algorithm on the 802.16a standard.

Finally, the thesis tested the performance of the 802.16a standard in various channels and the effect of various techniques such as interleaving, soft decision decoding, and diversity. Diversity is another area of current research as it has the ability to significantly improved system performance. The 802.16a standard provides for the use of Space-Time Coding (STC) transmit diversity, which can combine with various receiver diversity schemes. This thesis tested STC with maximal ratio combining (MRC) receiver diversity. Both of these are antenna or spatial diversity schemes. These schemes use multiple uncorrelated antennas. The resulting performance revealed significant improvements, allowing for much higher throughput.

I. INTRODUCTION

The IEEE 802.16a wireless standard was released in 2003 [1]. As the prevalence of wireless internet increases, its scale is also increasing. The 802.16 standard provides high bandwidth services to the metropolitan area. These wireless metropolitan area networks (WirelessMANs) provide fixed broadband point–to–multipoint access. These WMANs could also be used on the battlefield to provide higher bandwidth services for more functionality. Since 802.16a uses orthogonal frequency division multiplexing (OFDM), subcarriers that receive intentional interference can be modulated with "dummy" symbols in order for the system to continue functioning without modification at the receiver. In conjunction with 802.11 and 802.15, 802.16 provides wireless service for multiple local area networks (LANs) or wireless area networks (WANs). [2]

The increase of broadband internet in the last several years has led to the development of different methods of providing such bandwidth to customers. The popular definition describes broadband as having data rates above 1.5 Mbps. Currently, the primary providers are cable and digital subscribers lines (DSLs). Both, however, require a certain amount of infrastructure. IEEE's 802.16 standard is the wireless answer to broadband. With the current growth in wireless internet, 802.16 brings maturity to the broadband wireless realm in order to compete with its wired equivalents of DSL, cable, fiber optics, etc.

Taking advantage of the recently commercially available Orthogonal Frequency Division Multiplexing technique, 802.16a is able to provide robust broadband service. With the realization of Fast Fourier Transform (FFT) techniques on chips, the complexity of OFDM has dropped significantly. OFDM effectively implements parallel bit transmission. Since the adjacent frequency–multiplexed carriers are orthogonal, overlapping the carriers does not cause inter–carrier interference (ICI). This significantly increases the spectral efficiency while retaining resistance to fading and other occurrences in any real–world channel. [2]

Fading and multipath are two phenomena common to wireless channels. Both significantly distort the received signal and thus limit data rates. Fading can cause nulls

in certain portions of a signal's bandwidth, which would cause errors due to pulse mis-shaping. If the bandwidth were narrow enough, the entire signal could be lost. [3]

Multipath effectively spreads out a signal's duration over time due to varying path lengths between a receiver and a transmitter. If the bit length is short enough, or the multipath severe enough, the received power for a bit can continue into the next bit time causing inter–symbol interference (ISI). OFDM combats multipath by sending multiple bits in parallel; the actual length of each bit can be increased in order to receive as much power as possible from multipath. [3]

Since the carriers are so tightly overlapped, OFDM is especially sensitive to frequency and timing offsets among the carriers. Such offsets create a loss of orthogonality and therefore cause ICI. Pilot tones are thus introduced and training sequences are used to estimate the channel and provide known references within the OFDM symbol. The pilot tones help to correct frequency offsets that might occur due to sampling frequency and transmitter/receiver carrier frequency offsets. The channel impulse response will enable equalization at the receiver to combat fading. [2]

The 802.16a standard uses a form of transmitter diversity called Space–Time Coding (STC). Using two antennas, each symbol is transmitted twice (once on each antenna) with one of the transmissions being reformatted. These separate signals are then recovered by a single receiver antenna and combined using an estimation of the channel from the training sequence to calculate the transmitted signal. [1]

A. OBJECTIVE

Several techniques have been developed by [4] to reduce overhead in transmitting OFDM symbols for 802.11a. These were applied to the 802.16a standard to determine its performance, synchronization, and equalization. In addition, the STC technique used by the 802.16a standard was analyzed to combat fading and employ transmitter diversity.

B. THESIS OUTLINE

This thesis provides an overview of the 802.16a standard's physical layer as well as some aspects of fading channels and the concepts of OFDM and its use.

The thesis is organized into the follow chapters:

Chapter II discusses the channel model used to analyze the standard as well as an overview of the standard's physical layer, in particular Chapters 8 and 10 of [1].

Chapter III provides an overview of several synchronization techniques used for OFDM networks. These techniques include packet detection, clock estimation, time synchronization, and channel estimation. In addition, the technique of using only the short preamble for time and frequency synchronization as proposed by [4] is applied to 802.16a.

Chapter IV discusses channel coding and the Space–Time Coding (STC) technique optionally employed by 802.16a. In particular, Reed–Solomon and convolutional codes with hard and soft decision Viterbi decoding and block interleavers are discussed. Evaluated data are also included to determine the effect of the various techniques on system performance.

Chapter V provides a summary of the research done and recommendations for future work.

THIS PAGE INTENTIONALLY LEFT BLANK

II. BACKGROUND

Since 802.16a operates in the 2–11 GHz range, multipath and non–line of sight (LOS) signals can still provide significant energy to a received signal. In addition, noise must be added to accurately reflect any real–world system. Therefore, a channel model must be selected that accurately reflects the actual environment in which 802.16a will be employed. Since non–LOS channels experience greater fading and spreading than an LOS channel, combating multipath and fading takes on added importance. The channel model described in this chapter helps statistically to predict what types of distortions and attenuation the signal will experience between transmitter and receiver, which enables measures to be taken to mitigate its effects.

Noise is typically referred to as Additive White Gaussian Noise (AWGN). It is mathematically represented as a Gaussian variable added onto the signal at the receiver. In addition, interference from the channel causes the received signal power to vary in amplitude and sometimes frequency. Since one of the significant differences between the 10–66 GHz–band 802.16 and the 2–11 GHz 802.16a is the attenuation in its multipath, the worst–case scenario of no LOS is used and modeled as a Rayleigh random variable. Both variables are discussed in this chapter and used to determine their effects on the 802.16a signal.

This chapter also provides an overview of the 802.16a physical layer (PHY) in the 2–11 GHz band. The standard incorporates three primary modes of operation, which are single carrier (SCa), OFDM, and OFDMA (Orthogonal Frequency Division Multiple Access).

A. CHANNEL MODEL

In any wireless channel, there are several propagation effects that corrupt a signal. They are reflection, diffraction, and scattering. The physical entities and their location generally affect how much of each they experience. Metrics are used to determine the effect that the channel has on a signal and to provide a quantitative measure. These metrics determine what sort of measures should be employed and the severity of the signal's

distortion. These signal distortions include signal attenuation, time spread, and frequency spread. AWGN further deforms the signal at the receiver. [3]

The purpose of channel models is to mathematically calculate the statistical average of the effects upon the signal. Since channels generally change with time, the specific effects at any one time cannot be predicted except through stochastic, or random, variables. Therefore, for the amplitude A of a given signal, the faded value would be the expected value of A, $E\{A\}$. [3] Given the purpose of using non–LOS communications in employing 802.16a, a Rayleigh fading channel model was employed.

1. Multipath Fading

Fading differs from noise in that objects in the channel create the distortion, while noise is generated physically in the receiver. While every communications device experiences AWGN, the type of fading experienced across a communications channel changes based upon the conditions. The scope of the fading also decides how it is defined mathematically, whether it is large–scale propagation loss or small–scale fading. Several parameters help define the quality of the wireless channel: the rms delay spread, the coherence bandwidth, and the Doppler spread or coherence time. Table 1 illustrates their relation in defining a wireless channel. Coherence bandwidth and rms delay spread combine to characterize whether the channel is flat or frequency–selective fading. The Doppler spread and coherence time define whether the channel is fast or slow fading. [3]

Small-Scale Fading (based on multipath delay spread)	
Frequency Non-Selective (Flat) Fading	Frequency Selective Fading
1. BW of Signal < Coherence BW of channel 2. Delay Spread < Symbol Period	1. BW of Signal > Coherence BW of channel 2. Delay Spread > Symbol Period

Small-Scale Fading (based on Doppler spread)	
Fast Fading	Slow Fading
1. High Doppler Spread 2. Coherence Time < Symbol Period 3. Channel Varies Faster than Baseband Signal Variations	1. Low Doppler Spread 2. Coherence Time > Symbol Period 3. Channel Varies Slower than Baseband Signal Variations

Table 1. Types of Small–Scale Fading (After Ref. [3].)

a. Large–Scale Propagation Loss

Propagation loss attenuates a signal's strength based upon distance, height, and frequency. Large–scale loss defines the effects of reflection, diffraction, and scattering. Since the IEEE 802.16 standard will be employed in systems mostly in the urban and suburban areas, an appropriate model for attenuation of a signal versus distance must be selected. The well–known Okumura–Hata model only extends to 2 GHz with modification, and the IEEE 802.16 Broadband Wireless Access Working Group found that the model does not work well with low base-station (BS) heights and hilly or moderately– or heavily–wooded landscapes [3, 5]. The COST 231 Walfish–Ikegami model was proposed for flat suburban areas and urban areas with uniform building height [5].

b. Small–Scale Fading

Since any actual wireless channel is dynamic, small–scale fading is not a deterministic process. Instead, it is stochastic, meaning that the signal's amplitude cannot be given by an equation as in the Okomura–Hata model but can only be defined in terms of probabilities and statistical averages. [6]

The rms delay spread defines the standard deviation of the power-delay profile, or the delays of the arrivals of a given signal due to multipath reflection. A power-delay profile is the result of transmitting a narrow pulse at a transmitter and measuring the arrival time and amplitudes of the received pulses. If a channel is wide sense stationary or time-invariant, then the channel impulse response can be represented by [3]

$$h(\tau) = \sum_{i=0}^{N-1} a_i \exp(j\theta_i)\delta(\tau - \tau_i), \tag{2.1}$$

where a_i and θ_i are the amplitude and phase of the *i*-th signal and δ is the Kronecker delta function. The power-delay profile is then given as [3]

$$P(\tau) = \overline{k\left|h(\tau)\right|^2}. \tag{2.2}$$

The power-delay profile is typically an average of many samples over a local area to simulate the channel as time–invariant. [3]

The mean excess delay is given by [3]

$$\bar{\tau} = \frac{\sum_k a_k^2 \tau_k}{\sum_k a_k^2}, \tag{2.3}$$

where a_k is the signal amplitude at the given time τ_k. The rms delay spread, as the square root of the second central moment becomes [3]

$$\sigma_\tau = \sqrt{\frac{\sum_k a_k^2 \tau_k}{\sum_k a_k^2} - \bar{\tau}^2}. \tag{2.4}$$

The coherence bandwidth represents the bandwidth of a channel over which the relative attenuation is roughly equal or "flat." In other words, the bandwidth signifies high correlation of signal strength for two different frequencies. Two rules of thumb are given below for correlations of 0.9 and 0.5, respectively, [3]

$$B_c \approx \frac{1}{50\sigma_\tau} \tag{2.5}$$

and

$$B_c \approx \frac{1}{5\sigma_\tau}. \tag{2.6}$$

Doppler spread represents the frequency shift in a channel due to movement of the receiver, transmitter, or objects in the channel. It causes frequency dispersion due to the increase or decrease of the signal around the transmitted frequency. The variable B_D represents the Doppler spread and is the inverse of the coherence time T_C. The coherence time denotes the time over which the channel impulse response is time invariant. Therefore, the amplitude of two signals in that time period will have a high correlation The geometric mean of the coherence time, a common metric, is given by [3]

$$T_C = \sqrt{\frac{9}{16\pi f_m^2}} = \frac{0.423}{f_m}, \tag{2.7}$$

where f_m is the maximum Doppler shift. [3]

As seen in Table 1, a channel is flat or frequency–selective fading, depending upon the relation of both the signal's bandwidth to the coherence bandwidth and the symbol period to the delay spread. A channel is also considered to be slow or fast fading, depending upon a symbol period's relation to the coherence time. A fast fading channel will have a high Doppler spread. Both parameters define how quickly the channel's impulse response is changing. [3]

c. Rayleigh Fading Model

IEEE 802.16a systems are fixed, meaning that the Doppler spread will be extremely low since the receiver and transmitter are not moving [2]. Fixed location results in a relatively long coherence time, allowing for the longer bit times of parallel (OFDM) transmission. Therefore, a slow fading channel model would accurately resemble a typical channel that an 802.16a system might encounter. [5]

The coherence bandwidth metric outlines one of OFDM's primary advantages in terms of fading channels. RMS delay spreads in outdoor environments have values varying from 100 ns to 5.3 μs [5]. These values yield coherence bandwidths between 188.7 kHz and 10 MHz. Assuming worst–case scenario, a coherence bandwidth of 188 kHz would cause a highly–frequency selective fading channel for a single–carrier transmission of 7 MHz, which is a valid single–carrier 802.16a bandwidth. An OFDM symbol, however, with 200 subcarriers taking up a total of 7 MHz would have individual bandwidths of 35 kHz, meaning that each carrier's signal operated in a flat fading channel [1]. Therefore, each subcarrier's symbol would be uniformly attenuated in the frequency domain.

The Rayleigh random variable represents non–LOS channels where multipath elements would prevail. A typical instance would be when the BS antenna is no higher than the surrounding obstacles. Since no direct signal component is present, the incoming signal envelope has the Rayleigh distribution [6]. The Rayleigh probability density function (pdf) of the signal envelope is given as follows [7]

$$p(z) = \frac{z}{\sigma_0^2} e^{-\frac{z^2}{2\sigma_0^2}} \qquad z \geq 0, \tag{2.8}$$

where $2\sigma^2 = \mathrm{E}\left\{r^2\right\}$. Rayleigh fading serves as a worst–case scenario for multipath fading since there is no line–of–sight component. [6]

B. 802.16A OVERVIEW

Wireless broadband commonly refers to signals with data rates in excess of 1.5 Mbps. With high–speed internet becoming increasingly prevalent, infrastructure must keep up in order to connect end users (both commercial and private) to the backbone networks. There are four recognized methods: DSL, cable, wireless, and fiber optics. DSL and cable have the largest market penetration due to fully developed technologies. Both, however, require a fair amount of infrastructure in order to provide that service to customers. Cable requires a TV connection, and DSL can only extend 18,000 feet or so from a telephone company's office. Fiber optics costs too much to install in residential areas. As such, broadband wireless access (BWA), along with the overall wireless internet trend, offers significant potential for high–speed internet access with relatively little infrastructure. [2]

Developed in 1999 and approved in 2001, the 802.16 standard provides broadband internet access for the 10–66 GHz range. Since the frequencies are so high, attenuation is significant for non–LOS signals due to terrain and channel interference. At the same time, the higher attenuation and rain loss creates a need for higher link margins. [1]

In 2003, the 802.16a standard was released as an addendum to the 802.16 standard for the 2–11 GHz range. With the longer wavelength, 802.16a can receive non–LOS communication and therefore needs more advance power management techniques to lessen interference and to deal with channel changes. In addition, the 2–11 GHz range provides unlicensed bands. Therefore, these bands also need enhanced power management due to other users and power restrictions. [2]

1. 802.16 Architecture

Broadband wireless internet's architecture resembles that of cellular networks. Base stations (BS) provide the link between core networks and subscriber stations (SS). Therefore, the BSs provide point–to–multipoint (PMP) service in order to service multi-

ple SSs. Also, frequency reuse is utilized extensively as in cellular systems. The 802.16 standard also allows for mesh, or multipoint–to–multipoint (MP–MP), technology, which allows SSs to route information separately from the BS. BSs will often employ sectorized, directional antennas and even allow for adaptive antenna systems (AAS) to dynamically steer antenna beams based upon the number of users in the cell and their respective signal quality. [2]

Since data flows in both directions, multiplexing methods must be used in order to successfully transfer data. The downlink (DL) is from the BS to the SS, while the uplink (UL) is from SS to BS. The 802.16 standard employs frequency–division duplexing (FDD) and time–division duplexing (TDD) in order to separate the uplink from the downlink. Figures 1 and 2 provide examples of each type of duplexing. Notice the adaptive asymmetry between uplink and downlink subframes in the TDD mode. [1]

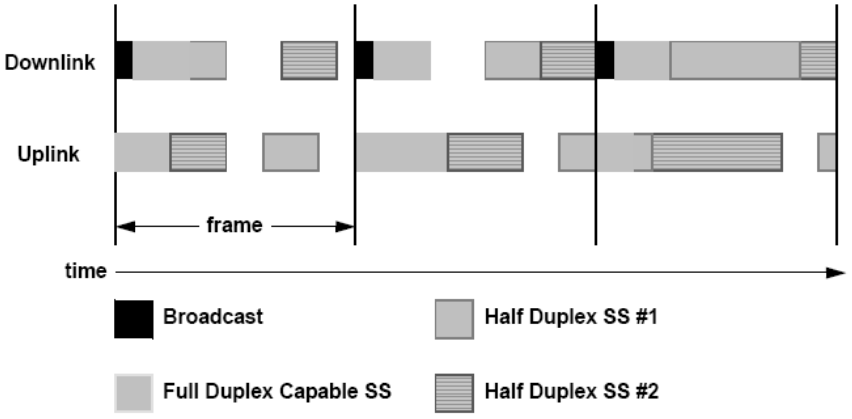

Figure 1. Example of FDD (From Ref. [1].)

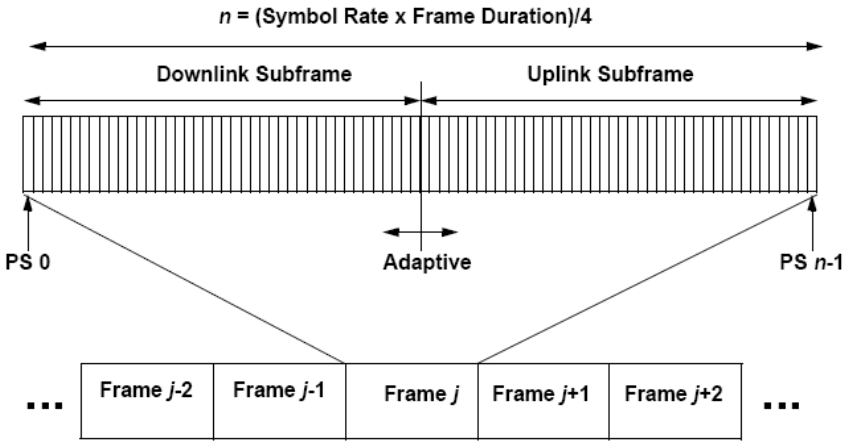

Figure 2. Example of TDD (From Ref. [1].)

2. MAC Layer

Figure 3 shows the relation between the MAC and PHY sublayers as well as the service access points. The MAC layer has three sublayers, each shown in the figure below. The MAC layer is connection–oriented and controls the multiple access schemes that support multiple users. This control includes the uplink and the downlink as well. Such controls include ranging to determine the delay of signal arrival for each of the SSs as well as UL and DL MAP (UL–MAP, DL–MAP) messages in order to define bursts start times. The MAC layer also controls quality–of–service (QoS) and security issues. [1]

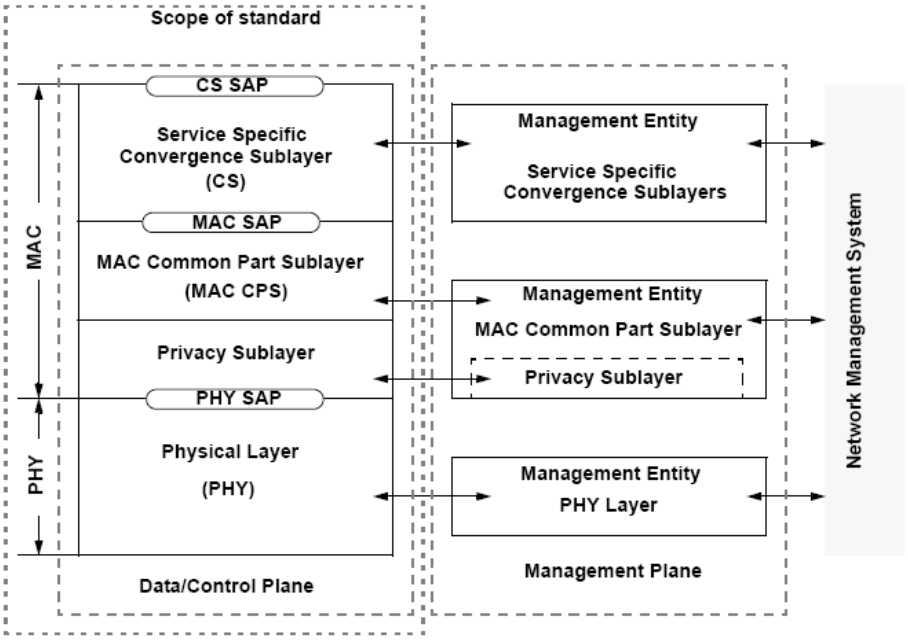

Figure 3. IEEE 802.16 Protocol Structure showing SAP's (From Ref. [1].)

3. 802.16a PHY Overview

The 802.16a physical layer's purpose is to transmit MAC layer messages. It has two sublayers, which are a transmission convergence sublayer and the Physical Medium Dependent sublayer. The MAC layer accesses the PHY via service access points (SAP) to transmit its messages, which the PHY sends as "primitives." These signals are all sent wirelessly in the 2–11 GHz frequency band. The 802.16a PHY has several modes of operation and prescribes the following three methods of transmitting and receiving data: [1]

- Single–Carrier (SCa)
- OFDM
- OFDMA

a. WirelessMAN – SCa

The 802.16a–SCa PHY transmits all data using a single carrier [1]. Since it is the only method that does not use OFDM, it has a number of different schemes for tracking phase error, transmit diversity, and generating a burst preamble among others.

The SCa burst frame in Figure 4 depicts the burst preamble. Many burst frames makes up the overall UL or DL subframe. The preamble contains a ramp-up pe-

riod followed by the preamble itself. The preamble is composed of a number of Unique Words. The ramp-up period consists of the last number of symbols of a Unique Word equal to the ramp-up time. Unique Words possess CAZAC (Constant Amplitude Zero [periodic] Auto–Correlation) properties and are derived from either Chu or Frank–Zadoff sequences. These words help provide channel estimation and should extend as long as the estimated delay spread. [1]

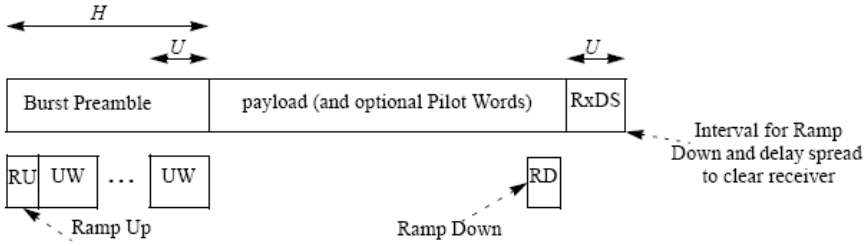

Figure 4. SCa Burst Frame (From Ref. [1].)

Following the preamble is the payload, which carries data and Pilot Words. Pilot Words are also composed of an integer number of Unique Words. A payload word consists of *F* symbols. Within each of those *F* symbols, *P* of them shall be for the optional Pilot Word. When Pilot Words are being transmitted, *F* is constant for the entire burst and the first pilot symbol transmitted is *F*–*P*+1 symbols into the burst and ceases when there are *F*–*P* or fewer symbols left. [1]

The burst frame ends with the ramp down and receiver delay spread clearing region (RxDS). The RxDS provides the receiver the ability to collect delayed signal elements due to multipath. The region can be set to zero; otherwise, the transmitter simply inserts zeros into the filter input. [1]

Single–carrier mode allows for several modulation schemes and coding rates not supported in OFDM transmission. In particular, SCa has the option to use 256–QAM and a 7/8 code rate. SCa also uses a TCM coder, as shown in Figure 5. As such, the output constellation is not a Gray code. TCM codes differ from Gray codes in that the adjacent constellation point differs by more than one bit. TCM coding applies only to QAM, since QPSK and BPSK inherently produce Gray codes. Figure 6 shows the constellation for 16–QAM. If no FEC is being used (optional), then only Gray codes are

used. Two optional methods of FEC are Block-Turbo Coding and Convolutional Turbo Coding. [1]

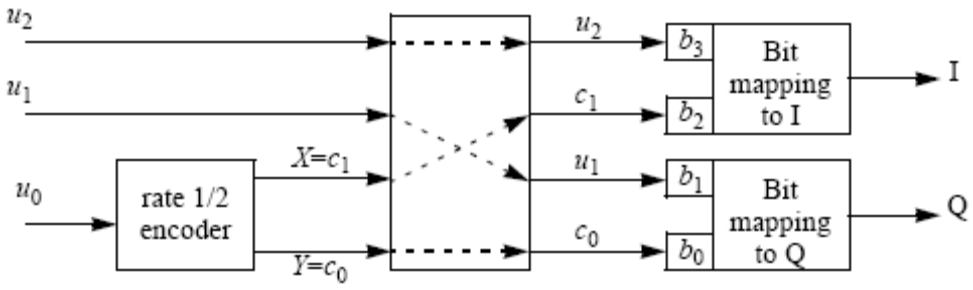

Figure 5. TCM Coder for Rate 3/4 16–QAM (From Ref. [1].)

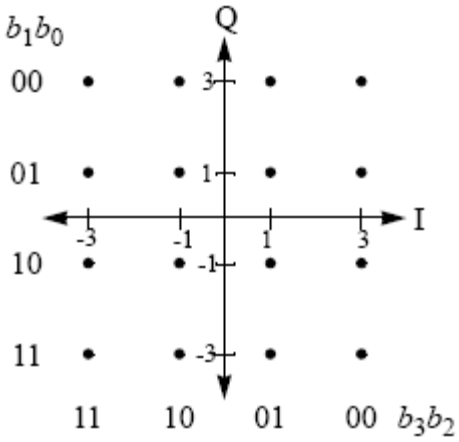

Figure 6. TCM Constellation for 16–QAM (From Ref. [1].)

Space–Time Coding (STC) is a form of transmit diversity employed in 802.16a. Using two transmit antennas, frames are sent twice, once on each antenna. They are then combined at the receiver and decoded using estimates of the channels. Single–carrier's employment of STC differs somewhat from that of OFDM. Figure 7 illustrates the combining of blocks into pairs in preparation for STC. Table 2 illustrates how each frame is sent on each antenna. Antenna 0 sends the data as usual with the addition of the delay spread guard. The order of the blocks is reversed from antenna 1 and its conjugate or negative conjugate is taken. [1]

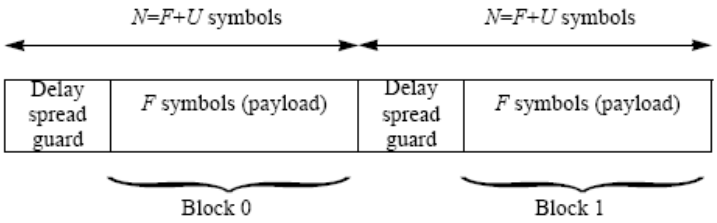

Figure 7. Paired Blocks for STC Transmit Diversity Combining (From Ref. [1].)

Tx Antenna	Block 0	Block 1
0	$\{s_0[n]\}$	$\{s_1[n]\}$
1	$\{-s_1^*[(F-n) mod(F))]\}$	$\{s_0^*[(F-n) mod(F))]\}$

Table 2. STC Transmission for SCa (From Ref. [1].)

The following equations demonstrate how to combine the received signals with their respective channel estimates $H_0(e^{j\omega})$ and $H_1(e^{j\omega})$ to decode STC. $C_0(e^{j\omega})$ and $C_1(e^{j\omega})$ are the decoded blocks so that [1]

$$\begin{aligned} R_0(e^{j\omega}) &= H_0(e^{j\omega})S_0(e^{j\omega}) - H_1(e^{j\omega})S_1^*(e^{j\omega}) + N_0(e^{j\omega}) \\ R_1(e^{j\omega}) &= H_0(e^{j\omega})S_1(e^{j\omega}) + H_1(e^{j\omega})S_0^*(e^{j\omega}) + N_1(e^{j\omega}) \end{aligned} \tag{2.9}$$

and, then,

$$\begin{aligned} C_0(e^{j\omega}) &= H_0^*(e^{j\omega})R_0(e^{j\omega}) + H_1(e^{j\omega})R_1^*(e^{j\omega}) \\ C_1(e^{j\omega}) &= -H_1(e^{j\omega})R_0^*(e^{j\omega}) + H_0^*(e^{j\omega})R_1(e^{j\omega}). \end{aligned} \tag{2.10}$$

b. WirelessMAN – OFDM

Orthogonal Frequency Division Multiplexing was not commercially viable until recently with the advent of chips that can perform the Fast Fourier Transform (FFT). The FFT algorithm enables bits to be placed onto orthogonal carriers using only one chip and one local oscillator. The chip essentially prepares the symbol in the frequency domain and then performs the IFFT to output the time signal. OFDM provides a method of transmitting bits in parallel, which greatly enhances the throughput of any system. Therefore, OFDM is generally regarded as the preferred method of modulation for

broadband systems that are being developed today. Since the bits are being transmitted in parallel, each bit length can be longer for the same bit rate, thereby reducing the fading effects of the channel. In addition, a cyclic prefix is added to the beginning of each symbol in order to mitigate the effects of multipath and delay spread in a channel. Since each data symbol is modulated on a different subcarrier, the transmitted signal becomes [1]

$$s(t) = \mathrm{Re}\left\{ e^{j2\pi f_c t} \sum_{\substack{k=-N_{used}/2 \\ k\neq 0}}^{N_{used}/2} c_k \cdot e^{j2\pi k\Delta f\,(t-T_g)} \right\}, \qquad (2.11)$$

where c_k is the modulated symbol, Δf is f_{sample}/N_{FFT}, and T_g is the length of the cyclic prefix. The OFDM portion of 802.16a is the focus of this study. Table 3 provides several parameters of WirelessMAN–OFDM. The N_{FFT} indicates the number of subcarriers in each OFDM symbol. As can be seen, only 200 carriers are actually used, with eight of those being pilot carriers. [1]

Parameter	Value
N_{FFT}	256
N_{used}	200
F_s / BW	licensed channel bandwidths which are multiples of 1.75 MHz and license-exempt: 8/7 any other bandwidth: 7/6
(T_g / T_b)	1/4, 1/8, 1/16, 1/32
Number of lower frequency guard carriers	28
Number of higher frequency guard carriers	27
Frequency offset indices of guard carriers	−128,−127...,−101 +101,+102,...,127
Frequency offset indices of BasicFixedLocationPilots	−84,−60,−36,−12,12,36,60,84
Subchannel number: Allocated frequency offset indices of carriers	1:{−88,...,−76},{−50,...,−39},{1,...,13},{64,...,75} 2:{−63,...,−51},{−25,...−14},{26,...,38},{89,...,100} 3:{−100,...,−89},{−38,...,−26},{14,...,25},{51,...,63} 4:{−75,...,−64},{−13,...,−1},{39,...,50},{76,...,88}

Table 3. OFDM Symbol Parameters (From Ref. [1].)

Since OFDM uses pilot carriers, pilot symbols can be sent continuously as opposed to single–carrier mode when pilot words must be sent periodically for synchronization and phase tracking. The pilot symbols are derived from a pseudorandom se-

quence with each carrier transmitting the same symbol. Details of WirelessMAN–OFDM are discussed later. [1]

c. WirelessMAN – OFDMA

WirelessMAN–Orthogonal Frequency Division Multiple Access (OFDMA) provides for multiple users by dividing the various subcarriers into subchannels. Figure 8 illustrates several subchannels. Since data shall be divided among subchannels, OFDMA symbols will not only be mapped in the time domain but will be mapped to the particular subchannel on which each symbol will be transmitted, resulting in a two–dimensional "data region." [1]

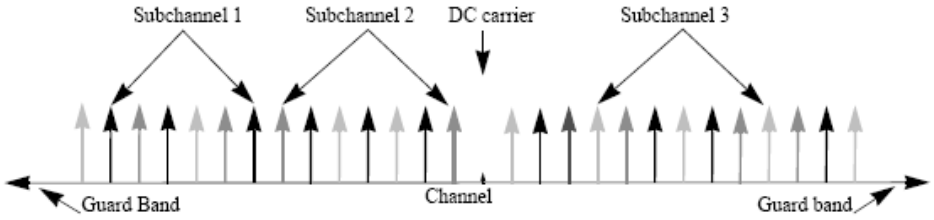

Figure 8. OFDMA Frequency Domain and Subchannels (From Ref. [1].)

A sample TDD frame is provided in Figure 9. Notice the several subchannels and the different transmissions made on each subchannel. One or more subchannels may be assigned to a SS, while the BS can selectively transmit subchannels. Since multiple users are to be supported, the number of FFT operations, and therefore subcarriers, is 2,048 as shown in Table 4. Along with the increased number of subcarriers, OFDMA employs variable location pilot carriers. The variable location pilots change carrier every symbol and repeat every four symbols according to the follow equation

$$varLocPilot_k = 3L + 12P_k, \tag{2.12}$$

where L is the modulo–4 index and P_k is the index of the appropriate pilot carrier. [1]

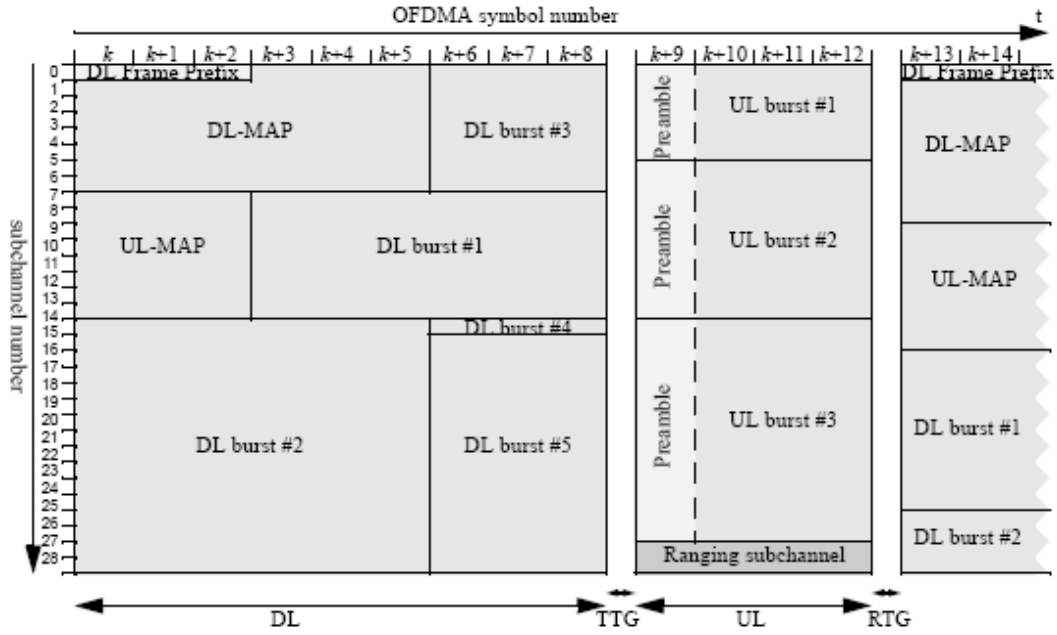

Figure 9. Sample OFDMA TDD Frame (From Ref. [1].)

Parameter	Value
Number of dc carriers	1
Number of guard carriers, left	173
Number of guard carriers, right	172
N_{used}, Number of used carriers	1702
Total number of carriers	2048
$N_{varLocPilots}$	142
Number of fixed-location pilots	32
Number of variable-location pilots which coincide with fixed-location pilots	8
Total number of pilots[a]	166
Number of data carriers	1536
$N_{subchannels}$	32
$N_{subcarriers}$	48
Number of data carriers per subchannel	48
BasicFixedLocationPilots	{0,39, 261, 330, 342, 351, 522, 636, 645, 651, 708, 726, 756, 792, 849, 855, 918, 1017, 1143, 1155, 1158, 1185, 1206, 1260, 1407, 1419,1428, 1461, 1530,1545, 1572, 1701}
$\{PermutationBase_0\}$	{3, 18, 2, 8, 16, 10, 11, 15, 26, 22, 6, 9, 27, 20, 25, 1, 29, 7, 21, 5, 28, 31, 23, 17, 4, 24, 0, 13, 12, 19, 14, 30}

Table 4. OFMA DL Carrier Allocations (From Ref. [1].)

C. SUMMARY

This chapter presented the importance of an accurate channel model to represent a channel mathematically. In addition to the ever–present AWGN, Rayleigh fading, without a direct signal path, serves as a worst–case scenario. Since 802.16a SSs are fixed, a channel is likely to be slow fading. By employing OFDM and reducing the bandwidth of the individual carrier, 802.16a can also "create" flat–fading channels.

An overview of the different modulation methods used by 802.16a was discussed. The standard can employ a traditional single–carrier mode with higher data rate options to make up for the lack of parallel bit transmission. It also allows for both OFDM and OFDMA in order to support different numbers of users. This study focuses on the OFDM mode of 802.16a in a Rayleigh fading channel.

Since the OFDM subcarriers are tightly overlapped, offsets in frequency and time can cause significant performance loss. Therefore, the signal must be properly synchronized. The next chapter deals with several aspects of synchronization of an OFDM symbol.

III. SYNCHRONIZATION

This chapter presents methods for synchronization of the packet. These include packet detection with and without preamble, time synchronization of OFDM symbols to determine when to start the DFT, frequency synchronization of subcarriers, carrier phase tracking, channel estimation, and equalization to reduce the effect of ISI.

Any communication system can perform only as well as it can synchronize. As such, the ability for a receiver to successfully detect an incoming signal even in poor conditions is essential. The signal must also be detected rapidly in order for the receiver to successfully decode the signal without missing any information. This is known as *single–shot synchronization* and comes from the packet–switched nature of the standard and the high data rates involved [4]. While 802.16a will ideally rely on timing to expect an incoming signal, as in cellular systems, its preamble provides the ability to synchronize should the timing signal fail [1].

One essential assumption is that the channel impulse response (CIR) remains the same for the duration of one packet. In 802.16a that must only hold for one subframe since both the DL and the UL transmit a preamble [1]. Each subframe is short enough to justify the assumption. The assumption is further justified due to the fixed nature of both transmitter and receiver [4].

A. THE 802.16A PREAMBLE

The 802.16a preamble is the means by which a receiver synchronizes with an incoming signal. The preamble also provides a means of estimating the wireless channel as discussed later. By transmitting a known sequence, the receiver can wait for the given sequence and start its timing of the signal based upon the arrival of the preamble. Two preambles exist in 802.16a. The short preamble, as shown in Figure10, is used by the uplink (UL), the downlink (DL) after the initial frame, and all adaptive antenna system (AAS) portions. It uses 50 subcarriers and consists of a cyclic prefix (CP) followed by two sequences of 128 samples. Equation (3.1) displays the frequency domain of the two–by–128 samples. The two square roots of two account for both the RMS power and a 3-dB boost. As in all the OFDM symbols, the time domain is achieved by taking the IFFT

of the sequence and adding to the beginning the last several samples to form the CP. The default length for the CP is 64 samples. [1]

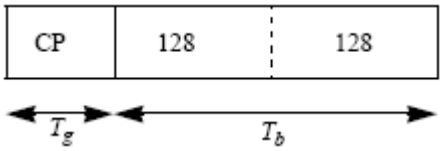

Figure 10. Short Preamble (From Ref [1].)

$$
\begin{aligned}
S(-100{:}100) = \{&+1+j, 0, 0, 0, +1+j, 0, 0, 0, +1+j, 0, 0, 0, +1-j, 0, 0, 0, -1+j, 0, 0, 0, +1+j, 0, 0, 0,\\
&+1+j, 0, 0, 0, +1+j, 0, 0, 0, +1-j, 0, 0, 0, -1+j, 0, 0, 0, +1+j, 0, 0, 0, +1+j, 0, 0, 0,\\
&+1+j, 0, 0, 0, +1-j, 0, 0, 0, -1+j, 0, 0, 0, +1-j, 0, 0, 0, +1-j, 0, 0, 0, +1-j, 0, 0, 0,\\
&-1-j, 0, 0, 0, +1+j, 0, 0, 0, -1+j, 0, 0, 0, -1+j, 0, 0, 0, -1+j, 0, 0, 0, +1+j, 0, 0, 0,\\
&-1-j, 0, 0, 0, 0, 0, 0, 0, -1-j, 0, 0, 0, +1-j, 0, 0, 0, +1+j, 0, 0, 0, -1-j, 0, 0, 0, -1+j,\\
&0, 0, 0, +1-j, 0, 0, 0, +1+j, 0, 0, 0, -1+j, 0, 0, 0, +1-j, 0, 0, 0, -1-j, 0, 0, 0, +1+j,\\
&0, 0, 0, -1+j, 0, 0, 0, -1-j, 0, 0, 0, +1+j, 0, 0, 0, +1-j, 0, 0, 0, -1-j, 0, 0, 0, +1-j,\\
&0, 0, 0, +1+j, 0, 0, 0, -1-j, 0, 0, 0, -1+j, 0, 0, 0, -1+j, 0, 0, 0, -1-j, 0, 0, 0, +1-j,\\
&0, 0, 0, -1+j, 0, 0, 0, +1+j\} * \sqrt{2} * \sqrt{2}.
\end{aligned}
\tag{3.1}
$$

The long preamble consists of an additional CP and four repetitions of 64 samples, as shown in Figure 11. The frequency domain of the four by 64 samples, which uses 100 subcarriers, is in Equation (3.2).

$$
\begin{aligned}
P1(-100:100) = \{&1, 0, -1, 0, -1, 0, -1, 0, 1, 0, 1, 0, 1, 0, 1, 0, -1, 0, 1, 0, -1,\\
&0, -1, 0, -1, 0, 1, 0, -1, 0, 1, 0, 1, 0, 1, 0, 1, 0, -1, 0, 1, 0, 1, 0, 1, 0, -1, 0, 1, 0,\\
&-1, 0, 1, 0, 1, 0, -1, 0, -1, 0, 1, 0, -1, 0, 1, 0, -1, 0, 1, 0, 1, 0, -1, 0, 1,\\
&0, 1, 0, -1, 0, -1, 0, -1, 0, 1, 0, -1, 0, -1, 0, -1, 0, -1, 0, -1, 0, 1, 0, 1, 0,\\
&0, [0]\\
&0, 1, 0, -1, 0, -1, 0, 1, 0, -1, 0, 1, 0, 1, 0, 1, 0, 1, 0, -1, 0, 1, 0, 1, 0,\\
&1, 0, 1, 0, -1, 0, 1, 0, -1, 0, -1, 0, -1, 0, -1, 0, 1, 0, 1, 0, -1, 0, 1, 0, -1,\\
&0, -1, 0, -1, 0, -1, 0, -1, 0, -1, 0, -1, 0, -1, 0, 1, 0, 1, 0, 1, 0, -1, 0, -1, 0,\\
&-1, 0, 1, 0, 1, 0, -1, 0, -1, 0, -1, 0, 1, 0, -1, 0, -1, 0, 1, 0, -1, 0, -1, 0, -1\} * \sqrt{2} * \sqrt{2}.
\end{aligned}
\tag{3.2}
$$

The long preamble is used as the initial DL preamble as well as for the initial ranging signal sent on the UL. The long preamble has the first sequence with four periods and the second sequence with two periods. [1]

Figure 12 shows the time domain sequence of the 128 samples for a bandwidth of 28 MHz with the 64 samples in Figure 13. The timing depends upon the bandwidth,

which defines the sampling frequency. The sampling frequency–to–bandwidth ratio for licensed bands is defined as [1]

$$\frac{f_s}{BW} = \frac{8}{7}. \tag{3.3}$$

For the licensed bandwidth of 28 MHz, the sampling frequency would be 32 MHz. [1]

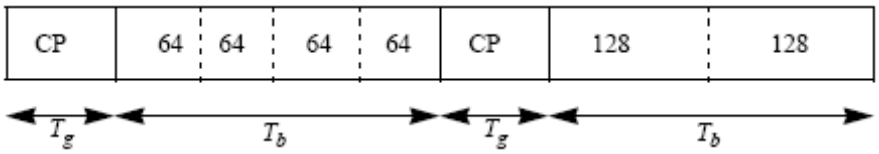

Figure 11. Long Preamble (From Ref [1].)

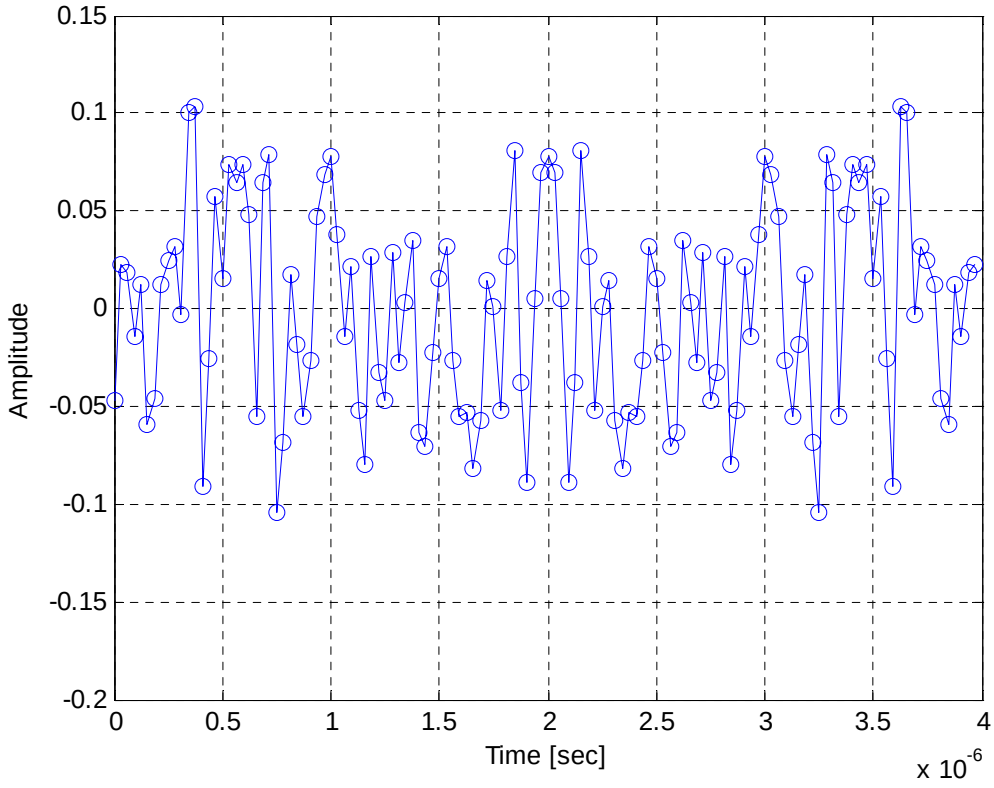

Figure 12. Sequence of 128 Samples (Real Part)

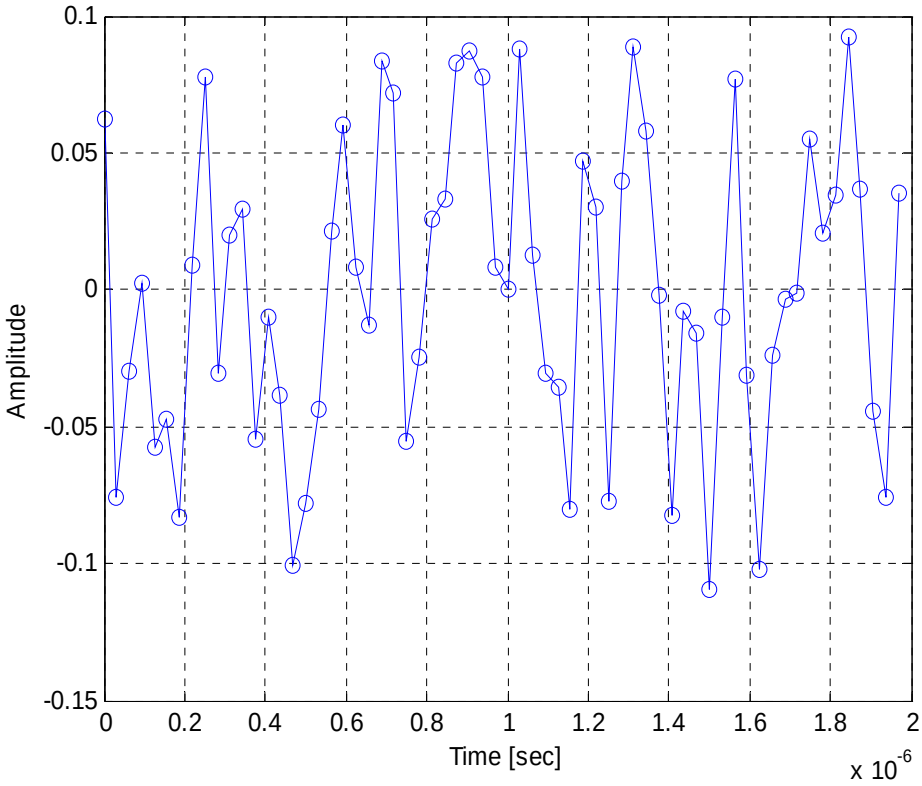

Figure 13. Sequence of 64 Samples (Real Part)

B. PACKET DETECTION

The rest of the packet decoding process depends upon rapid and accurate packet detection. Since the 802.16a standard operates as a cellular system, the times of the arrival of packets on the UL and DL are important and therefore drive the synchronization. All BSs are synchronized to a common timing signal to ensure accuracy at the BS. This common signal ensures frequency accuracy as well. The SS must transmit its symbol such that it arrives at its appropriate time within 50% of the minimum guard interval or better. Ideally, both the BS and SS should know when to expect an incoming signal. Nevertheless, the system must still be able to function should the timing signal fail. [1]

As with any metric, a threshold must be set in order to define when the packet is detected or is not detected. This decision statistic, m_n, creates two probabilities, which must be balanced to achieve maximum performance. The first probability is the probability that a packet is actually present, P_d. It must be balanced against the probability of a

false detection, P_{fd}. There is no severe error of a false detection, since the receiver will realize it after its first data integrity check, but the penalty of not detecting a present packet is lost data. [4]

1. Packet Detection with Preamble

The 802.16a preamble provides the receiver the ability to do a number of things including detect the packet's beginning. As in [8], using a *Delay and Correlate Algorithm* provides a way to detect the packet's start by taking advantage of the periodic nature of the symbols within the preamble. Figure 14 shows a block diagram of the algorithm.

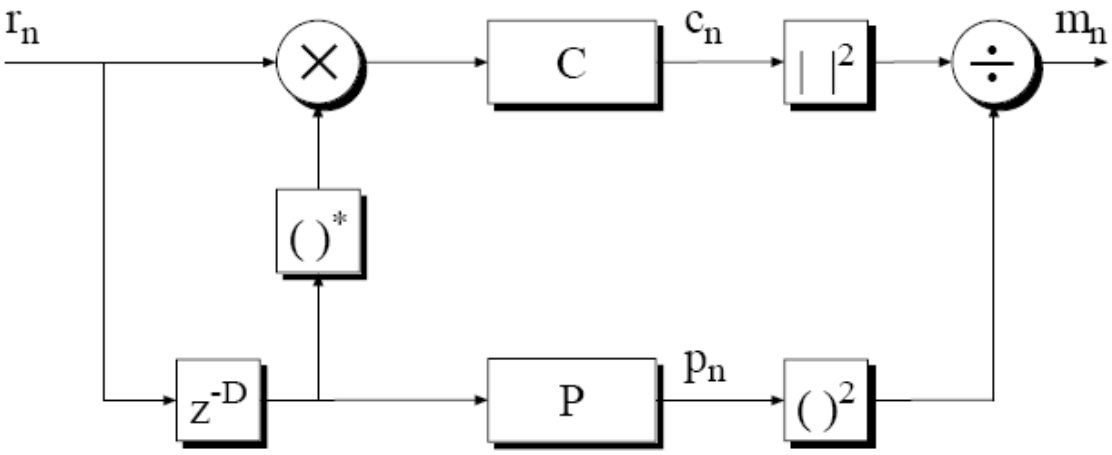

Figure 14. Block Diagram of Delay and Correlate Algorithm (From Ref. [4].)

The values c_n and p_n are given by the following equations:

$$c_n = \sum_{k=0}^{L-1} r_{n+k} r_{n+k+D}^{*} \tag{3.4}$$

and

$$p_n = \sum_{k=0}^{L-1} \left| r_{n+k+D} \right|^2 \tag{3.5}$$

where L is the search window length (i.e., the number of samples over which the algorithm will "search" for the preamble) and D is the delay. Block C provides the cross–correlation as seen in Equation (3.4). The delay is chosen to be the period of a sequence.

For 802.16a this would be 64 for the long preamble (4x64 samples) or 128 for the short preamble (2x128 samples). Block *P* measures the power and normalizes the decision statistic [4]. The decision statistic m_n is simply

$$m_n = \frac{|c_n|^2}{p_n^2}. \tag{3.6}$$

Figure 15 plots the decision statistic for a SNR of 0 dB. The long preamble was used with a delay *D*=192 samples to follow the periodicity of the four times 64 samples. The value of m_n jumps noticeably even at a low SNR since noise is uncorrelated and zero mean. The beginning of the packet is easily detectable.

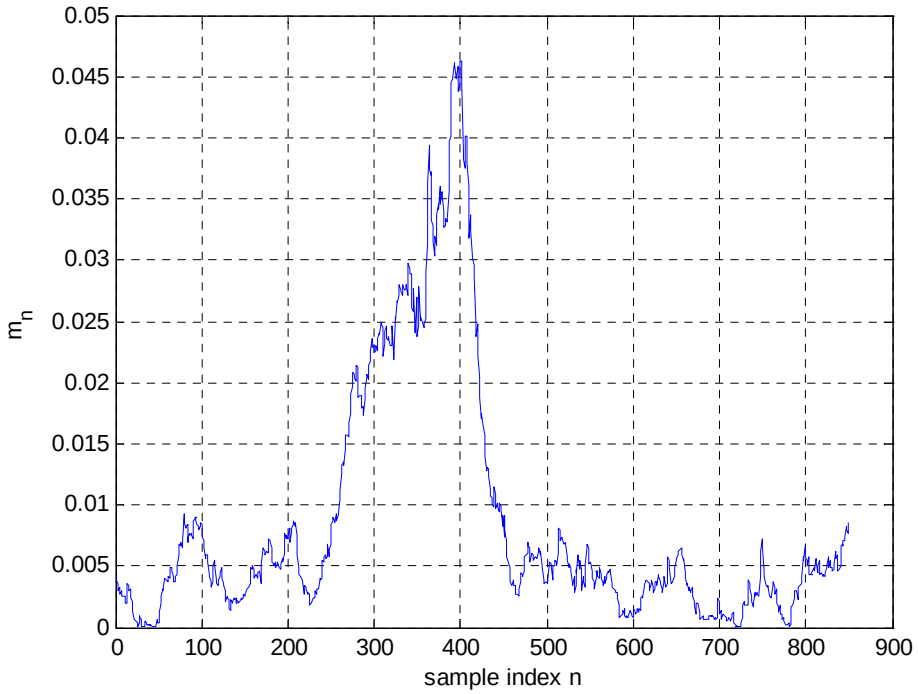

Figure 15. Packet Detection with Preamble (SNR = 0 dB)

2. Packet Detection without Preamble

If no preamble is present at the beginning of a symbol, the only method of detecting an incoming signal is to measure the power level. Therefore the decision statistic would look something like

$$m_n = \sum_{k=0}^{L-1} r_{n-k} r_{n-k}^{*} = \sum_{k=0}^{L-1} \left| r_{n-k} \right|^2 . \tag{3.7}$$

This method is generally unreliable as the amount of noise power is unknown and can vary significantly over time, making the setting of a dependable threshold difficult. [4]

C. TIME SYNCHRONIZATION

Time synchronization refers to the point at which the DFT begins in order to de-code the OFDM symbol. [4] As proposed in [8], OFDM systems can use a cross–correlation of a known reference signal (the preamble or a portion thereof) to determine when to start the DFT.

The beginning of the symbol is especially hard to determine in multipath fading. The CP in each OFDM symbol exists as a guard interval to deal with multipath. The CP is an extension of the end of the symbol at the beginning. Therefore, if the DFT is set early, it gets the last values of the symbol in the CP and discards the ones at the end of the symbol. A late DFT window, however, results in ISI due to the CP from the next OFDM symbol, as shown in Figure 16. [2]

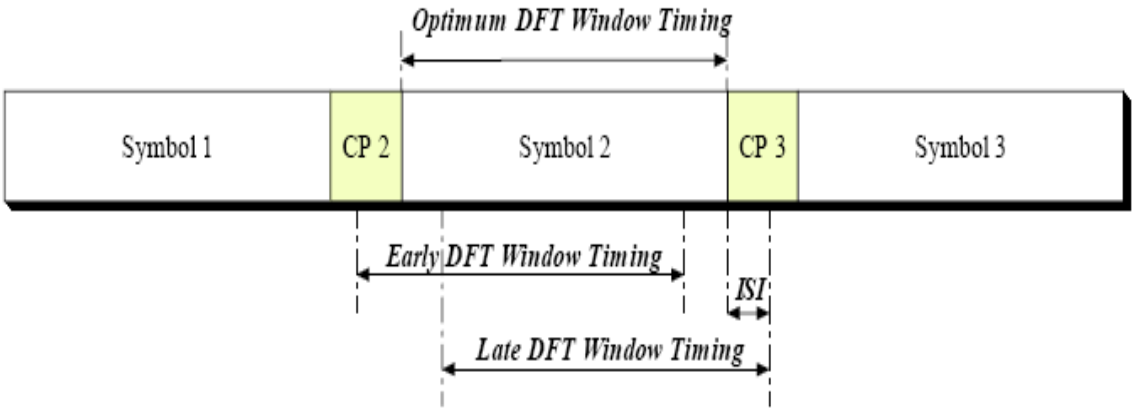

Figure 16. DFT Window Timing (From Ref. [4].)

D. FREQUENCY SYNCHRONIZATION

A serious drawback of OFDM is its sensitivity to carrier frequency offset. When a frequency offset is introduced, the system's performance is degraded by the reduction in amplitude of the offset carrier and the resulting loss of orthogonality causing ICI. [4, 9, 10] As seen in Figure 17, only when the carrier is sampled at its maximum amplitude is

there no ICI. In addition to frequency offset, phase noise $\theta(t)$, modeled as a Weiner process, can cause frequency offset. [9]

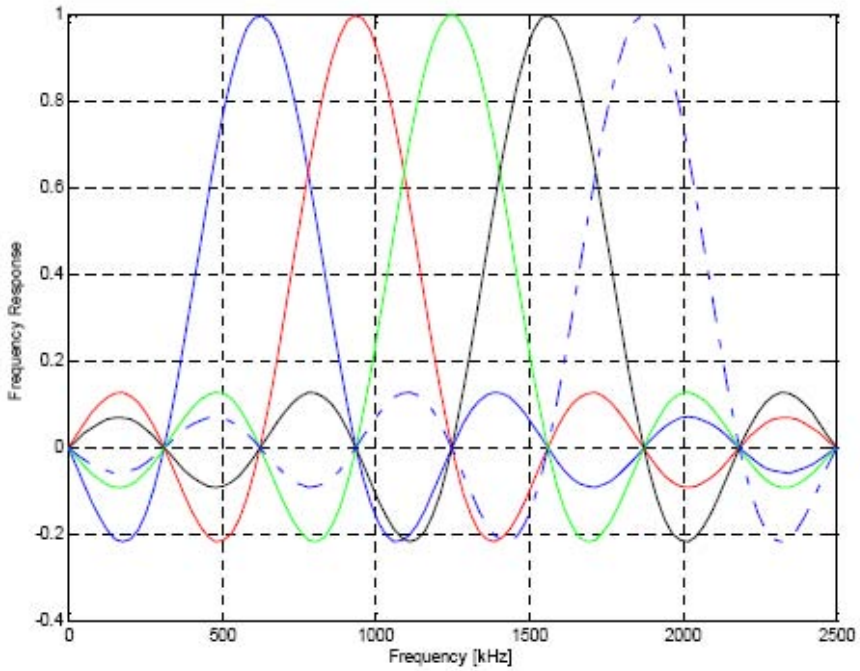

Figure 17. Overlapping Orthogonal Carriers (From Ref. [4].)

As shown in [4] and [9], the degradation due to carrier offset is given by

$$\Lambda[\text{db}] \cong \begin{cases} \dfrac{10}{\ln 10}\dfrac{1}{3}\left(\pi N \dfrac{\Delta F}{R}\right)^2 \dfrac{E_b}{N_0} & \text{OFDM} \\ \dfrac{10}{\ln 10}\dfrac{1}{3}\left(\pi \dfrac{\Delta F}{R}\right)^2 & \text{SC} \end{cases} \tag{3.8}$$

where R is the symbol rate and ΔF is the carrier offset. Equation (3.8) shows that the degradation in dB of the signal's SNR is proportional to the carrier offset squared and square of the number of subcarriers in the OFDM case. Therefore, 802.16a (200 subcarriers) will be much more sensitive to carrier offset than 802.11a (52 subcarriers) [1, 4].

In the case of phase noise, Λ is very similar with β as the local oscillator linewidth [9]

$$\Lambda[\text{db}] \cong \begin{cases} \dfrac{10}{\ln 10}\dfrac{11}{60}\left(4\pi N\dfrac{\beta}{R}\right)\dfrac{E_b}{N_0} & \text{OFDM} \\ \dfrac{10}{\ln 10}\dfrac{1}{60}\left(4\pi\dfrac{\beta}{R}\right)\dfrac{E_b}{N_0} & \text{SC} \ . \end{cases} \tag{3.9}$$

For 802.16a, the BS shall maintain frequency synchronization to within +/– 4 ppm for licensed bands, and the SS shall be synchronized with the base station to within two percent of carrier spacing. The standard mandates that the receiver SNR must not degrade by more than 0.5 dB relative to the transmitter SNR. [1]

1. Maximum Likelihood (ML) Estimation of Frequency Offset

The ML estimation of frequency offset requires the use of two identical OFDM symbols. [8, 10] The 802.16a preamble repeats several symbols allowing for the delay and correlation using the identical symbols. With a received signal of [4]

$$r_n = s_n e^{j2\pi\Delta f n T_s}, \tag{3.10}$$

where Δf is the carrier frequency offset between transmit and receipt and T_s is the sampling interval, the correlation with delay D becomes [4]

$$\begin{aligned} c &= \sum_{n=0}^{L-1} r_n r_{n+D}^* \\ &= \sum_{n=0}^{L-1} s_n e^{j2\pi\Delta f n T_s}\left(s_n e^{j2\pi\Delta f (n+D)T_s}\right)^* \\ &= \sum_{n=0}^{L-1} s_n s_n^* e^{j2\pi\Delta f n T_s} e^{-j2\pi\Delta f (n+D)T_s} \\ &= e^{-j2\pi\Delta f D T_s}\sum_{n=0}^{L-1}|s_n|^2. \end{aligned} \tag{3.11}$$

The frequency offset estimator then becomes [4]

$$\Delta f = -\frac{1}{2\pi D T_s}\text{angle}(c). \tag{3.12}$$

The estimation can also be done in the frequency domain using the DFT. The following represents the DFT of the first and second OFDM symbols received, respectively:

$$R_{1,k} = \sum_{n=0}^{N-1} r_n e^{-\frac{j2\pi kn}{N}} \qquad k = 0,1,\ldots,N-1 \tag{3.13}$$

$$\begin{aligned} R_{2,k} &= \sum_{n=N}^{2N-1} r_n e^{-\frac{j2\pi kn}{N}} \\ &= \sum_{n=0}^{N-1} r_{n+N} e^{-\frac{j2\pi kn}{N}} \qquad k = 0,1,\ldots,N-1 \end{aligned} \tag{3.14}$$

where k is the subcarrier index, and N is the total number of subcarriers. From [4] and [10], the second received symbol has the following relation to the first received OFDM symbol:

$$R_{2,k} = R_{1,k} e^{j2\pi f_\Delta} \tag{3.15}$$

meaning that each subcarrier experiences a shift proportional to the frequency offset. The value $f_\Delta = \Delta f / f_{sc}$ is the relative frequency offset to f_{sc}, which is the subcarrier spacing. Again, taking the correlation yields [4]

$$\begin{aligned} C &= \sum_{k=-K}^{K} R_{1,k} R_{2,k}^* \\ &= \sum_{k=-K}^{K} R_{1,k} \left(R_{1,k} e^{j2\pi f_\Delta} \right)^* \\ &= e^{-j2\pi f_\Delta} \sum_{k=-K}^{K} R_{1,k} R_{1,k}^* \\ &= e^{-j2\pi f_\Delta} \sum_{k=-K}^{K} \left| R_{1,k} \right|^2 \end{aligned} \tag{3.16}$$

and a frequency offset estimator of

$$\hat{f}_\Delta = -\frac{1}{2\pi} \text{angle}(C) \Leftrightarrow \Delta f = -\frac{f_{sc}}{2\pi} \text{angle}(C). \tag{3.17}$$

2. Properties of the ML Estimation Algorithm

The limitations of the algorithm are an important part to operating it and knowing its effectiveness. The phase shift is only unambiguous between the values of $\pm\pi$. [10] Therefore, the maximum offset is bounded by

$$\left|\Delta f\right| \le \frac{\pi}{2\pi DT_s} = \frac{1}{2DT_s}. \tag{3.18}$$

The 802.16a sampling time depends upon the bandwidth as in Equation (3.2), which yields different frequency limits on the offset depending upon the sampling time. Assuming a bandwidth of 28 MHz and a corresponding sampling frequency of 32 MHz, the maximum frequency offset for the 64 samples in the long preamble would be

$$\Delta f_{\max,64} = \frac{1}{(2)(64)\left(31.24\times10^{-9}\right)} = 250 \text{ kHz}. \tag{3.19}$$

For the short preamble with periodicity of 128, the maximum offset would be

$$\Delta f_{\max,128} = \frac{1}{(2)(128)\left(31.24\times10^{-9}\right)} = 125 \text{ kHz}. \tag{3.20}$$

For the smallest bandwidth of 1.75 MHz with a sampling frequency 2 MHz, each maximum offset becomes

$$\Delta f_{\max,64} = \frac{1}{(2)(64)\left(5\times10^{-7}\right)} = 15.625 \text{ kHz} \tag{3.21}$$

and

$$\Delta f_{\max,128} = \frac{1}{(2)(128)\left(5\times10^{-7}\right)} = 7812.5 \text{ Hz}. \tag{3.22}$$

Since the maximum frequency offset tolerated at the BS is 4 ppm in licensed bands, the maximum possible difference between BS and SS is 8 ppm, assuming maximum offsets with opposite signs [1]. The carrier frequency for 802.16a can also vary between 2–11 GHz. Therefore, the maximum transmit offset tolerated at the BS will vary between $\Delta f = \left(8\times10^{-6}\right)\left(2\times10^{9}\right) = 16$ kHz for a 2 GHz carrier and $\Delta f = \left(8\times10^{-6}\right)\left(11\times10^{9}\right) = 88$ kHz for a carrier frequency of 11 GHz. Thus, either preamble will be able to reliably resolve the maximum allowable frequency offset at the 28 MHz bandwidth but would not be able to resolve either at a bandwidth of 1.75 MHz.

Therefore, as in [4], the first half of the long preamble will provide coarse frequency estimation, and the second half will enable fine frequency synchronization.

E. COMBINED TIME AND FREQUENCY SYNCHRONIZATION

The synchronization method proposed in [4] uses the elements of the delay and correlate algorithm except that the window length *L* must be equal to the delay *D*, which must be one symbol length such that [4]

$$\begin{aligned} c_n &= \sum_{k=0}^{D-1} r_{n+k} r_{n+k+D}^{*} \\ p_n &= \sum_{k=0}^{D-1} \left| r_{n+k+D} \right|^2 . \end{aligned} \tag{3.23}$$

In hardware, the summations can be implemented to give only one complex multiplication per received sample as follows: [4]

$$\begin{aligned} c_{n+1} &= c_n + \left(r_{n+D} r_{n+2D}^{*} \right) - \left(r_{n-1} r_{n+D-1}^{*} \right) \\ p_{n+1} &= p_n + \left| r_{n+2D} \right|^2 - \left| r_{n+D-1} \right|^2 . \end{aligned} \tag{3.24}$$

The frequency offset estimator is the same as before

$$\Delta f = -\frac{1}{2\pi D T_s} \text{angle}(c_{n_0}) \tag{3.25}$$

where c_{n_0} is the corresponding cross–correlation of the index n_0 for the symbol timing estimate.

The 802.16a preamble repeats several sequences multiple times to allow this algorithm to work. Using the 4×64 sequences at the beginning of the long preamble, the system can both detect the packet and perform frequency synchronization. A flow chart of the algorithm is in Figure 18.

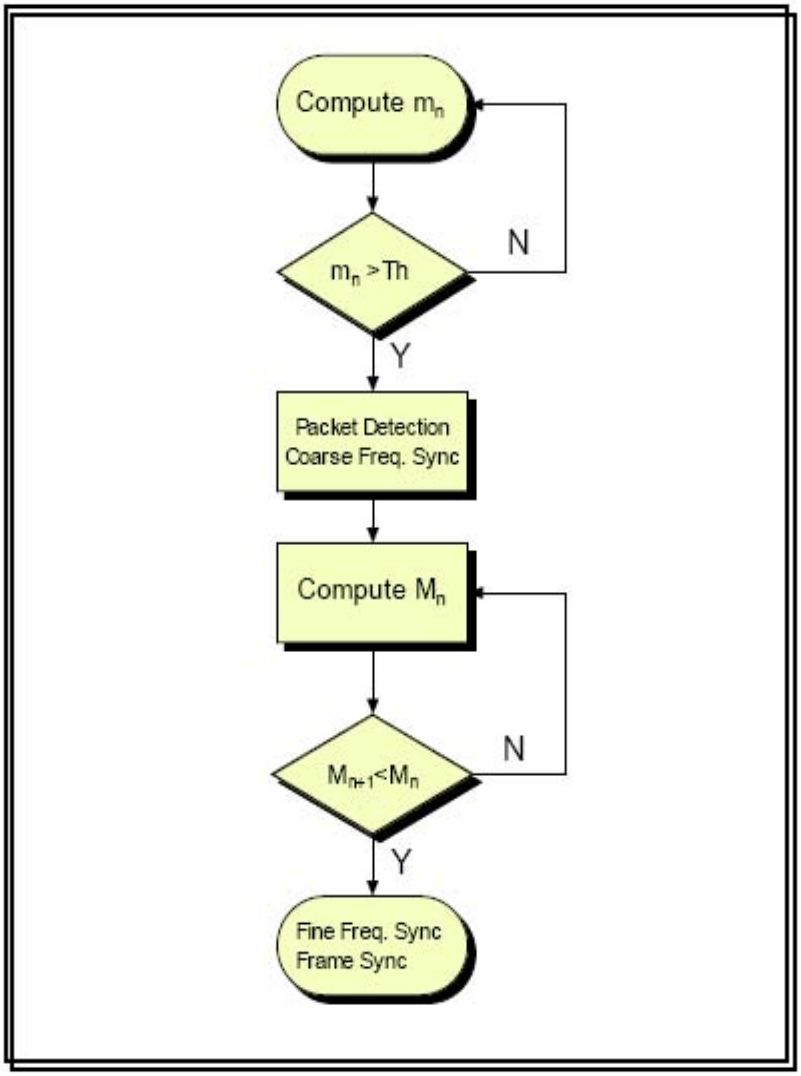

Figure 18. Flow Chart of the Combined Synchronization Algorithm (From Ref. [4].)

The decision statistic m_n, as above, is given by

$$m_n = \frac{|c_n|^2}{p_n{}^2}. \tag{3.26}$$

The following simulation shows the performance of the 802.16a standard in an AWGN channel with SNR = 10 dB, Δf = 80 kHz, and D = 192. The maximum frequency offset becomes 83.333 kHz, which cannot resolve the maximum tolerated frequency offset for a carrier of 11 GHz. Figure 19 shows the start of the packet at sample index 400. The simulation used the long preamble. The value of D = 192 was chosen since the correlation of the four repetitions of 64 samples correlates at the beginning of the packet, but

the two repetitions of 128 samples do not correlate so as to give two peaks, which appear when $D = 64$ or $D = 128$ are chosen.

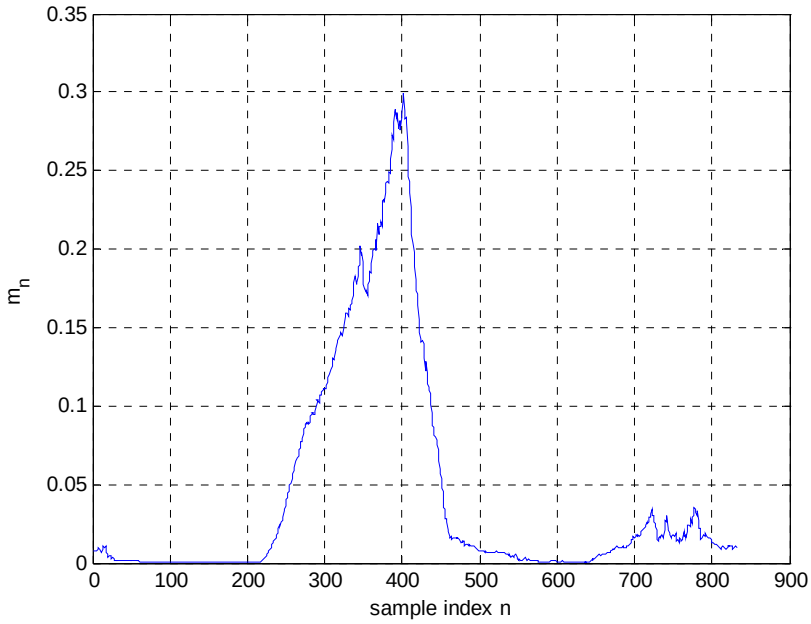

Figure 19. Decision Statistic m_n in AWGN Channel with SNR = 10 dB and $D = 192$

This simulation was run 10,000 times with the above settings. The simulation was also run in a Rayleigh fading channel with an RMS delay spread of 400 ns. Figures 20-23 provide histograms of the resulting timing and frequency offset estimates.

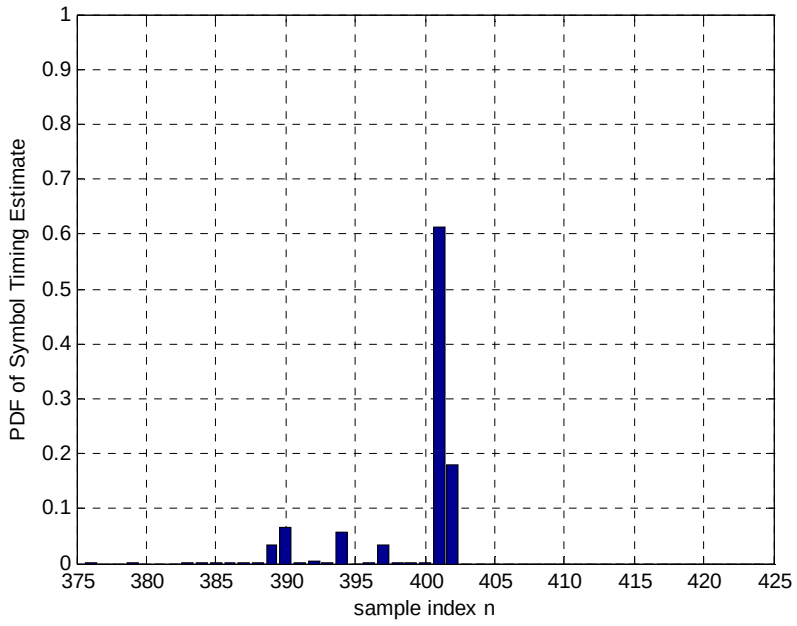

Figure 20. PDF of Symbol Timing Estimate in AWGN, SNR = 10 dB

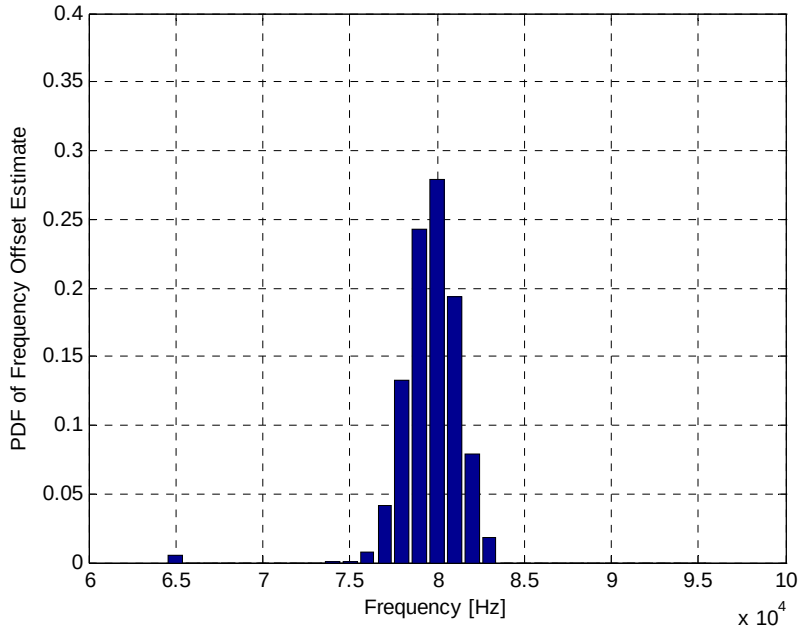

Figure 21. PDF of Frequency Offset Estimate in AWGN, SNR = 10 dB

The PDF of the symbol estimates reveals that, almost 80% of the time, the correct sample is chosen with one–sample precision. In addition, the frequency offset estimate

follows a normal distribution with distribution of 2 kHz. Since the carrier spacing for a 28-MHz bandwidth system is 128 kHz, the relative offset is $2\ \text{kHz}/128\ \text{kHz} \approx 0.0156$, which means that the relative offset is only 1.6% of the carrier spacing.

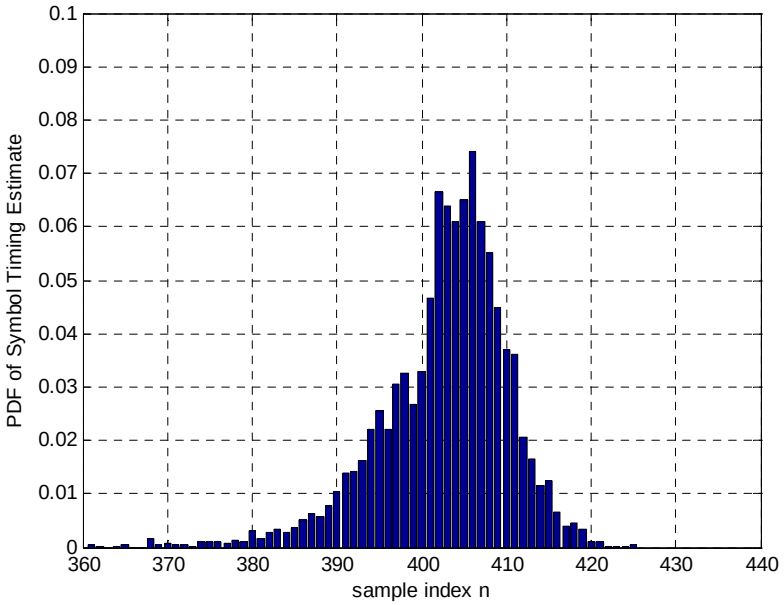

Figure 22. PDF of Symbol Timing Estimate in Rayleigh Fading Channel with RMS Delay Spread = 400 ns, SNR = 10 dB

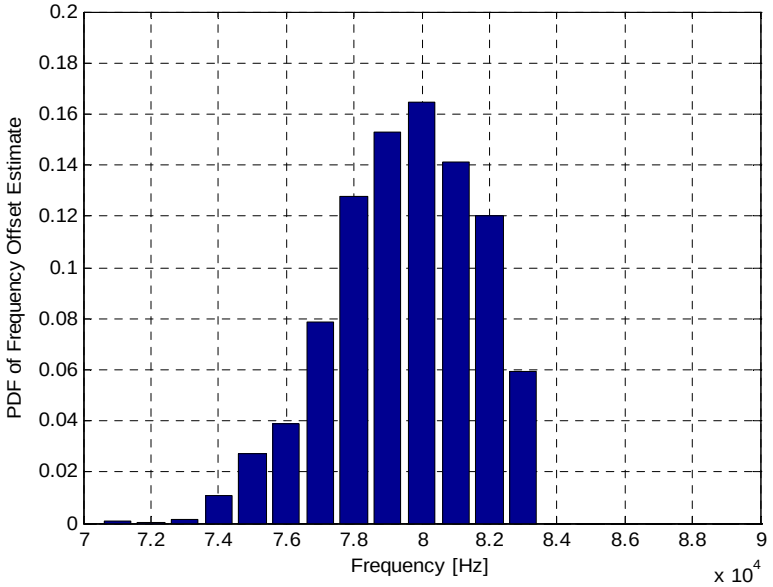

Figure 23. PDF of Frequency Offset Estimate in Rayleigh Fading Channel with RMS Delay Spread = 400 ns, SNR = 10 dB

As can be seen, the effect of fading causes significant deterioration in the algorithm. In addition, since the frequency offset was set near the resolvable limit, the frequency offset estimate exceeded the limit of 83.333 kHz, seen by the abrupt cutoff after 83 kHz. In more severe fading environments, the training sequence does not accurately resolve symbol synchronization. Since most of the power is non–LOS, the majority of the power from each pulse comes after the initial arrival. Therefore, the decision statistic m_n will reach a maximum value after the actual arrival of the packet.

The problem in obtaining an accurate symbol estimate is due to the similar periodicities of the two sequences. In the long preamble, using a delay of $D = 128$ will provide two spikes for each half of the preamble. A delay of $D = 64$ will provide several spikes in the first half of the preamble due to the four repetitions. Using $D = 192$ provides the single spike and, for longer RMS delay spreads, the shift in the DFT window can be increased to six or seven to account for the generally late estimation of the algorithm.

Since $D = 192$ cannot resolve the maximum frequency offset even with a maximum bandwidth, the coarse frequency synchronization can be performed using either $D = 64$ or $D = 128$. When the decision statistic passes the threshold, the $D = 192$ can then be used to provide fine synchronization. The two repetitions of 128 samples at the end of the long preamble can then be used for channel estimation. For the short preamble, the $D = 128$ is used for both since only the two repetitions of 128 samples are used.

F. CARRIER PHASE TRACKING

Since noise can never be eliminated, there will always be some error in terms of frequency offset estimation. While the ICI can be minimized to a negligible level, the frequency offset can never be eliminated. While this might not degrade the SNR substantially, the offset causes rotation in the modulation constellation. Therefore, after even only a few symbols, the constellation may have rotated due to the extra phase shift, as in Figure 24, to a point beyond the decision boundaries of each symbol making successful demodulation of the signal impossible. Therefore, the phase of the carriers must be tracked as well. [4]

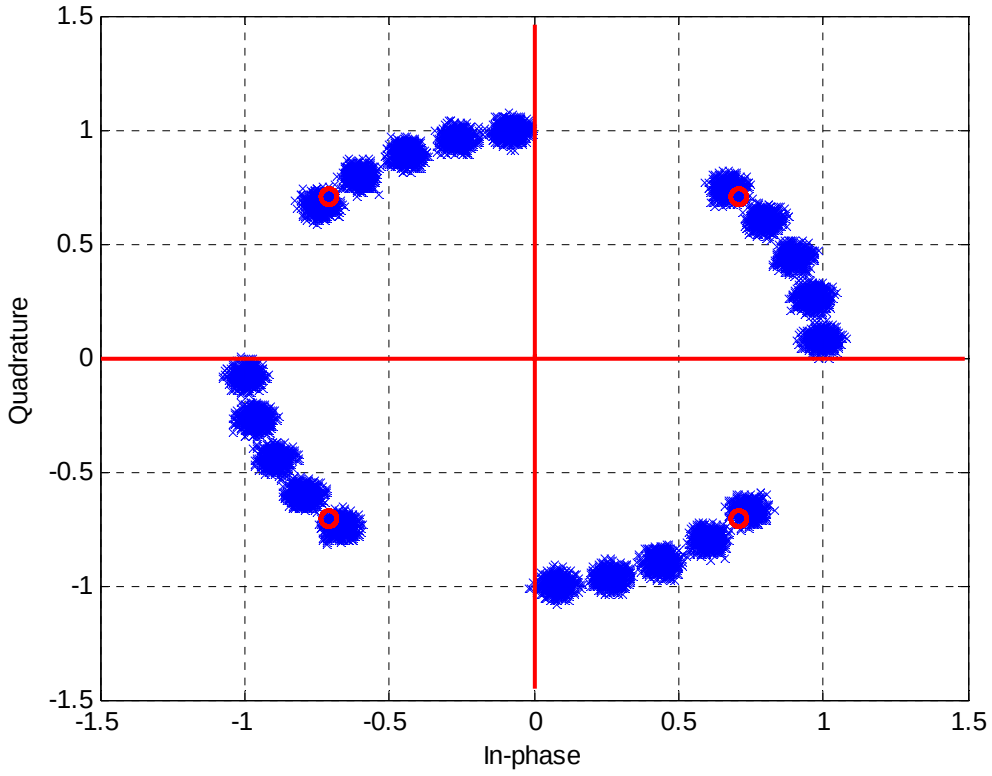

Figure 24. QPSK Constellation Rotation with 3-kHz Frequency Error

The general method for tracking carrier phase is via pilot symbols, of which 802.16a has eight. Since each carrier experiences the same phase shift, the phase shift experienced by the pilot symbols can be used to de–rotate the constellation for all the subcarriers. If the channel transfer function is H_k and the pilot symbol is $P_{1,k}$, the received signal becomes [4]

$$R_{1,k} = H_k P_{1,k} e^{j2\pi n f_\Delta}. \tag{3.27}$$

Therefore, the phase estimator is [4]

$$\begin{aligned} \hat{\Phi}_l &= \text{angle}\left[\sum_{k=1}^{N_p} R_{1,k}\left(\hat{H}_k P_{1,k}\right)^*\right] \\ &= \text{angle}\left[\sum_{k=1}^{N_p} H_k P_{1,k} e^{j2\pi n f_\Delta}\left(\hat{H}_k P_{1,k}\right)^*\right], \end{aligned} \tag{3.28}$$

where H_k^* is the channel estimate and N_p is the number of pilot subcarriers per OFDM symbol. Assuming a perfect channel estimate, the phase estimator becomes [4]

$$\begin{aligned}\hat{\Phi}_l &= \text{angle}\left[\sum_{k=1}^{N_p}\left|H_k\right|^2\left|P_{1,k}\right|^2 e^{j2\pi n f_\Delta}\right] \\ &= \text{angle}\left[e^{j2\pi n f_\Delta}\sum_{k=1}^{N_p}\left|H_k\right|^2\right]\end{aligned} \tag{3.29}$$

since $P_{1,k}$ is set equal to one [1]. In this case the signal can be fully de–rotated since the exact phase offset is known. Since a perfect channel estimate is not realizable, the phase estimator will also not fully de–rotate the constellation, further contributing to the phase noise.

G. CHANNEL ESTIMATION

Channel estimation seeks to define the transfer function of the channel. Since the channel is in general assumed to be time–invariant for a symbol length, the effect of the channel will be somewhat constant throughout that symbol length. Channel estimation is mandatory for 802.16a in order to handle constellation rotation, equalize, and reconstruct signals that are using diversity. [1] Channel estimation can be done in either the time or frequency domain.

1. Frequency Domain Method

The long preamble provides the sequence of two 128-sample sequences in order to allow for channel estimation. Each received symbol is the result of the channel transfer function and AWGN as shown: [4]

$$R_{l,k} = H_{l,k}X_{l,k} + W_{l,k} \quad l = 1,2, \qquad k = 0,1,...,K-1. \tag{3.30}$$

The number of subcarriers is *K*. The channel transfer function $\hat{H}_{l,k}$ is found simply by dividing by the training symbols like the following: [4]

$$\hat{H}_{l,k} = \frac{R_{l,k}}{X_{l,k}} = H_{l,k} + \frac{W_{l,k}}{X_{l,k}}. \tag{3.31}$$

Since AWGN is zero–mean, the average value of the $W_{l,k}$ term is zero. Therefore the channel can be estimated plus the noise found in the receiver. This technique is simple but does not take into account the correlation in the channel estimates. [4]

2. Time-Domain Method

In the time domain, the CIR is calculated. The actual CIR is circularly convolved with the transmitted signal, as shown below, and noise is added

$$r_{l,n} = h \otimes x_n + w_{l,n}. \tag{3.32}$$

Here, the value h denotes the CIR, $\otimes$ denotes convolution, x_n is the transmitted signal, and $w_{l,n}$ is AWGN.

Circular convolution can be performed using the matrix multiplication [4]

$$\mathbf{r} = \mathbf{X}\mathbf{h} + \mathbf{w}, \tag{3.33}$$

where

$$\mathbf{X}=\begin{bmatrix} x_1 & x_{64} & \cdots & x_{64-L+2} \\ x_2 & x_1 & \cdots & x_{64-L+3} \\ \vdots & & \ddots & \vdots \\ x_{63} & x_{62} & \cdots & x_{64-L} \\ x_{64} & x_{63} & \cdots & x_{64-L+1} \end{bmatrix}, \quad \mathbf{h}=\begin{bmatrix} h_1 \\ h_2 \\ \vdots \\ h_{L-1} \\ h_L \end{bmatrix}, \quad \mathbf{w}=\begin{bmatrix} w_1 & w_2 & \cdots & w_{64} \end{bmatrix}^T. \tag{3.34}$$

The CIR estimate is then calculated using the $\mathbf{X}^\dagger$, which is the Moore–Penrose generalized inverse of $\mathbf{X}$ [11]. The channel estimate is as follows:

$$\begin{aligned} \hat{\mathbf{h}} &= \mathbf{X}^\dagger \left(\mathbf{r}_{\mathbf{1,n}} \right) \\ &= \mathbf{X}^\dagger (\mathbf{X}\mathbf{h} + \mathbf{w}_{\mathbf{1,n}}) \\ &= \mathbf{X}^\dagger \mathbf{X}\mathbf{h} + \mathbf{X}^\dagger \mathbf{w}_{\mathbf{1,n}} \\ &= \mathbf{h} + \mathbf{X}^\dagger \mathbf{w}_{\mathbf{1,n}}. \end{aligned} \tag{3.35}$$

The channel transfer function is simply the DFT of the CIR estimate.

H. EQUALIZATION

Given the signal below,

$$r_l = h_m \otimes s_n + w_l \qquad l = m + n - 1, \tag{3.36}$$

with $m < n$, the frequency domain is as follows: [4]

$$R_k = H_k S_k + W_k. \tag{3.37}$$

To equalize the signal, the channel estimate $\hat{H}_k$ is applied to the frequency domain received signal per the following equation:

$$R_{k,eq} = \frac{R_k}{\hat{H}_k} = \frac{H_k}{\hat{H}_k} S_k + \frac{W_k}{\hat{H}_k}. \tag{3.38}$$

Since the equalization uses only an estimation of the channel transfer function, the channel effects are not perfectly inverted. In addition, in some instances, dividing by the channel estimate will increase the noise amplitude. [4]

I. SUMMARY

Synchronization provides the basis of the performance of the rest of any OFDM system. Since OFDM is so sensitive to frequency and time offsets, effective, quick algorithms must be used to synchronize the system. Since the channel can generally be assumed to be stationary for the length of one symbol, the necessary time and frequency synchronization can be done in the preamble and applied to the rest of the symbol. This chapter covered an algorithm using the 802.16a preamble that detects the packet, synchronizes the symbol in the time domain, and corrects the frequency offset in each carrier. This can be done in the first half of the long preamble (four repetitions of 64 samples), while the second half (two repetitions of 128 samples) is used for channel estimation. Several simulations were run demonstrating the algorithm's performance in AWGN and Rayleigh fading. Brief discussions of carrier phase tracking, channel estimation, and equalization were provided. The first two are mandatory for most OFDM systems, including 802.16a.

The next chapter provides an overview of the 802.16a OFDM PHY frame, and its performance in various channels and with various types of coding applied.

THIS PAGE INTENTIONALLY LEFT BLANK

IV. PERFORMANCE OF 802.16A

This chapter discusses channel coding and the Space–Time Coding (STC) technique optionally employed by 802.16a. In particular, Reed–Solomon and convolutional codes with hard and soft decision Viterbi decoding and block interleavers are discussed. Evaluated data are also included to determine the effect of the various techniques on system performance.

A. OVERVIEW OF 802.16A FRAME AND TRANSMISSION PROCESS

The 802.16a standard supports two types of duplexing, Frequency Division Duplexing and Time Division Duplexing. These are for the purpose of separating DL and UL traffic. Using the PMP architecture, Figure 25 shows the design of a TDD frame. The FDD frame looks the same except that the DL and UL sections are transmitted at the same time but in different frequencies and there is no transmitter transition gap (TTG) or receiver transition gap (RTG). [1]

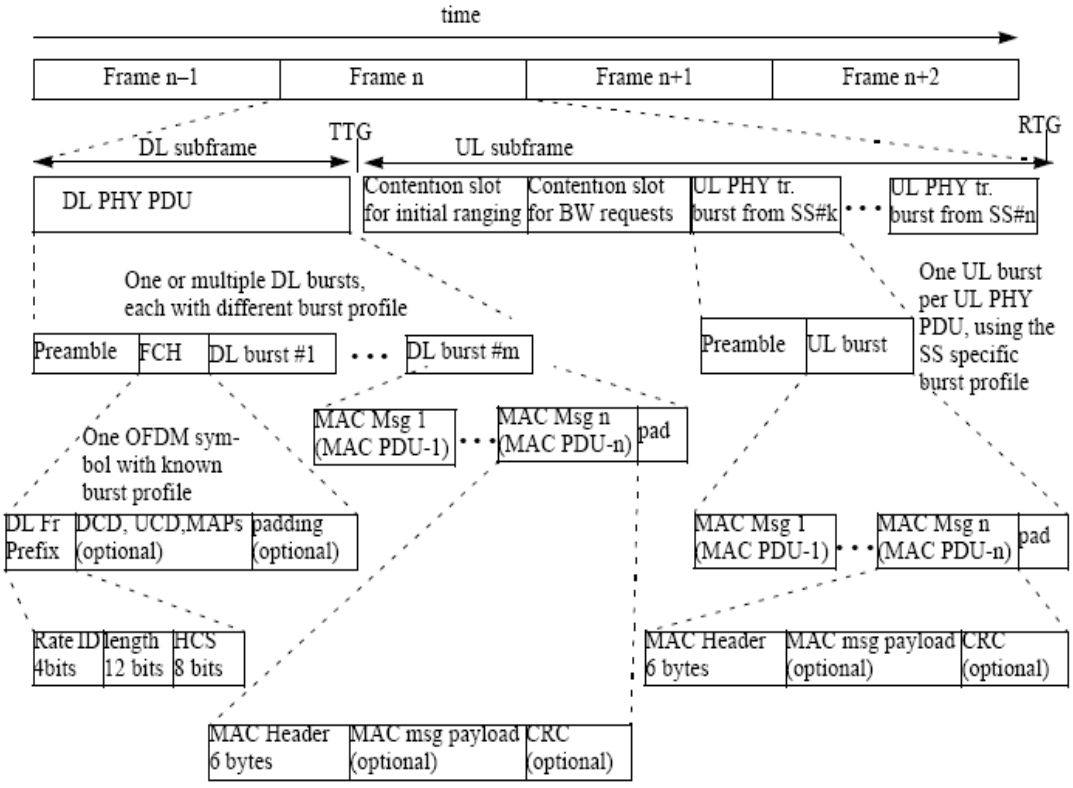

Figure 25. OFDM TDD Frame (From Ref. [1].)

The DL is from BS to SS, and the UL is from SS to BS. Each DL slot begins with a preamble followed by a Frame Control Header (FCH). The Frame Control Header contains information about the subframe's length, type of modulation used, whether diversity is used, etc. The FCH is followed by the DL bursts, which send data to several or individual SSs. The UL subframe has portions set up for ranging and additional bandwidth requests from SSs. The ranging slot allows each SS to know when to transmit so that its symbol arrives within its proper slot at the BS. The TTG and RTG allow for the collection of multipath and prevent interference between subframes at either end. [1]

Each frame is encoded in the manner provided in Figure 26. The DL supports QPSK and 16–QAM, with 64–QAM as an optional modulation scheme. Forward Error Correction (FEC) coding supports the rates 1/2, 2/3, 3/4, and 5/6. The data begins coding by being randomized in order to spectrally spread the signal. Next, the data is coded by blocks in the rate $r = 1/2$ Reed–Solomon code, which is not included in the simulations run to analyze the standard, followed by the convolutional encoder. Other rates are achieved by puncturing the codes. The bits are then interleaved in order to intersperse burst errors so that the Viterbi decoder can decode them. The appropriate number of bits is mapped onto each of the 192 data subcarriers of an OFDM symbol. Finally, each OFDM symbol is converted into the time domain via the IFFT algorithm and given a CP. Windowing is then performed to limit the OFDM symbol, and each symbol is attached one to another. [1, 2]

B. TRANSMITTER

Figure 26 shows the block diagram of the SCa transmitter for both the UL and the DL. All three methods begin the transmission process by randomizing incoming bits using a pseudorandom sequence. Figure 27 illustrates how the bits are randomized. The transmit process begins by randomizing the bits using a pseudorandom sequence. Only source bits (e.g., not frame control or pilot symbols) are randomized. The randomizer spectrally spreads the signal via modulo–2 addition of the source bits to the Linear–Feedback Shift Register (LFSR).

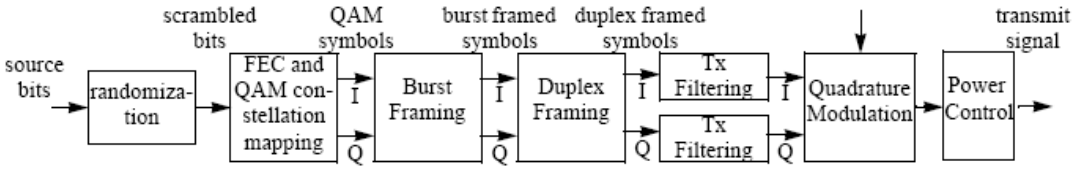

Figure 26. 802.16a PHY Transmitter (From Ref. [1].)

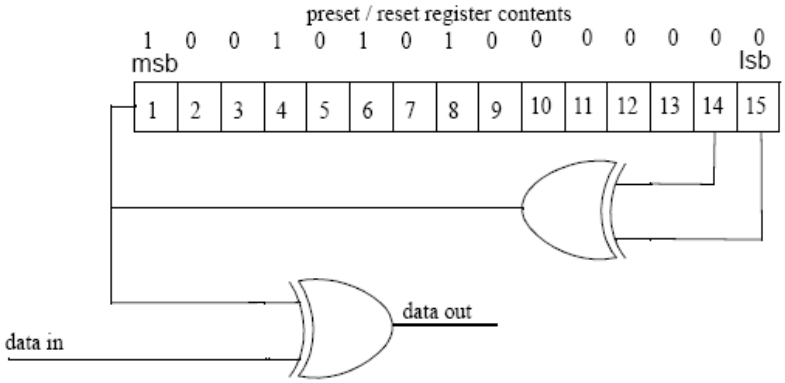

Figure 27. Bit Randomizer (From Ref. [1].)

The randomizer is followed by forward error correction (FEC). The 802.16 uses a concatenated code with a convolutional inner code and a Reed–Solomon (RS) outer code with a default rate of 1/2. The coding rate *r* denotes the number of coded bits to uncoded bits. It therefore describes how much longer a coded sequence will be than an uncoded sequence. The Reed–Solomon code is derived from a systematic RS $(N = 255, K = 239)$ code using GF(2^8), where *N* is the number of bytes after encoding, *K* is the number of bytes before encoding, and $R = N - K$ is the number of parity bytes. The code may be punctured to provide various code rates. An optional block interleaver can be used in between the RS code and the convolutional code. The code and field generator polynomials are as follows:

Code Generator Polynomial:

$$g(x) = (x + \lambda^0)(x + \lambda^1)(x + \lambda^2)..(x + \lambda^{2T-1}),\ \lambda = 02_{HEX} \tag{4.1}$$

Field Generator Polynomial

$$p(x) = x^8 + x^4 + x^3 + x^2 + 1. \tag{4.2}$$

The inner convolutional code has the block diagram depicted in Figure 28. The encoder has a rate of 1/2 and constraint length $K = 7$.

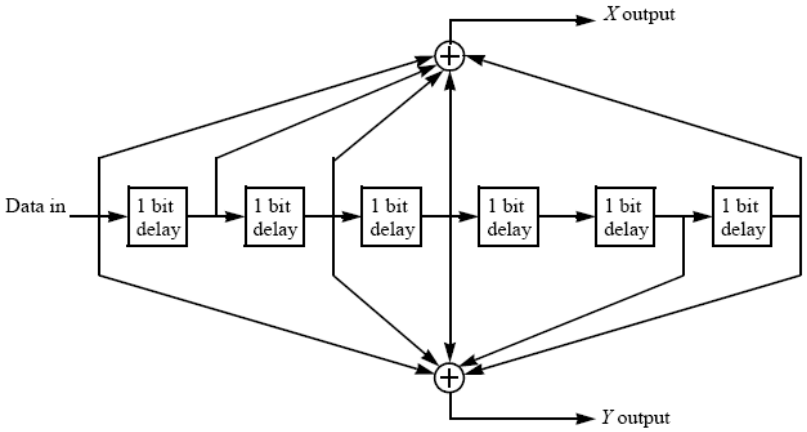

Figure 28. Binary rate 1/2 Convolutional Encoder (From Ref. [1].)

	Code rates			
Rate	1/2	2/3	3/4	5/6
d_{free}	10	6	5	4
X	1	10	101	10101
Y	1	11	110	11010
XY	X_1Y_1	$X_1Y_1Y_2$	$X_1Y_1Y_2X_3$	$X_1Y_1Y_2X_3Y_4X_5$

Table 5. OFDM Supported Punctured Code Rates (From Ref. [1].)

As in Table 5, the various r = 1/2 encoded sequences may be punctured to support other coding rates. The "0" represents a punctured bit and not the actual bit's value.

Modulation	Uncoded block size (bytes)	Coded block size (bytes)	Overall coding rate	RS code	CC code rate
QPSK	24	48	1/2	(32,24,4)	2/3
QPSK	36	48	3/4	(40,36,2)	5/6
16-QAM	48	96	1/2	(64,48,8)	2/3
16-QAM	72	96	3/4	(80,72,4)	5/6
64-QAM	96	144	2/3	(108,96,6)	3/4
64-QAM	108	144	3/4	(120,108,6)	5/6

Table 6. Mandatory Channel Coding per Modulation (From Ref. [1].)

After being randomized and encoded, the sequence is then interleaved. Since a channel impulse response is generally seen as time–invariant over a short amount of time, any interference introduced from the channel in a frequency band may produce bit errors for that duration. Therefore, many bit errors are "bursty", meaning that they affect an adjacent string of bits rather than evenly interspersed throughout the sequence. Since Viterbi decoders can only decode a certain number of errors per constraint length, an interleaver rearranges the order of the bits in order to intersperse bursty errors. In addition, it rearranges the adjacent bits so that they are not placed on adjacent carriers, which is a form of frequency diversity. The mathematic algorithm that interleaves the bits is given by [1]

$$m = (N_{cbps}/16)\cdot k_{\mathrm{mod}(16)} + \mathrm{floor}(k/16) \qquad k = 0,1,..,N_{cbps}-1 \tag{4.3}$$

$$j = s\cdot \mathrm{floor}(m/s) + \left(m + N_{cbps} - \mathrm{floor}(16\cdot m/N_{cbps})\right)_{\mathrm{mod}(s)} \quad m = 0,1,..,N_{cbps}-1. \tag{4.4}$$

The indexes *m* and *j* represent the data after the first and second permutations, respectively [1]. Figure 29 provides simulated results of data using Matlab coding with and without interleaving in a Rayleigh fading channel with a rms delay spread of 100 ns. The figure shows that interleaving significantly improves performance in a Rayleigh fading channel.

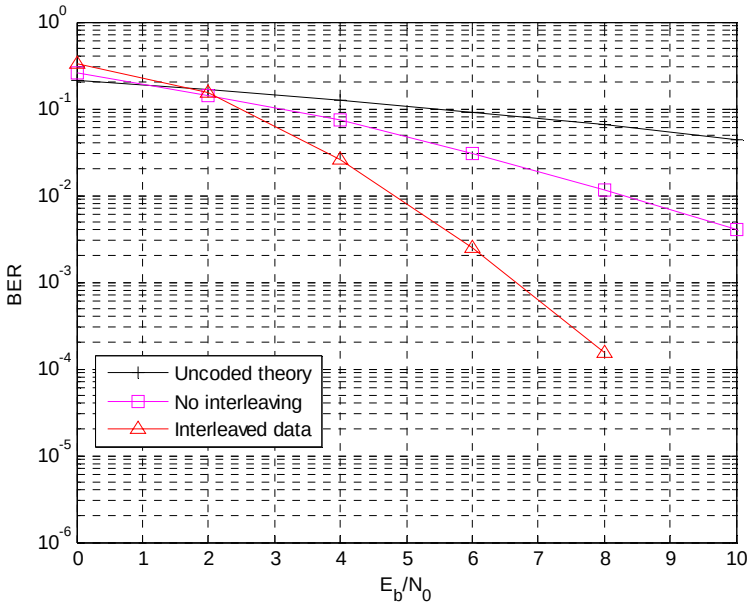

Figure 29. Bit Error Rate of IEEE 802.16a rate 1/2 QPSK with and without Interleaving in 200–ns RMS Delay Spread Rayleigh Fading Channel

The interleaved data is then mapped serially according to the modulation scheme selected. The first output carrier will be $-N_{FFT}/2$. The DL must support both QPSK and 16–QAM, with 64–QAM optional. Figure 30 shows the Gray code constellation for 16-QAM. In addition, the pilot carriers are given their symbols and inserted into the sequence. Each pilot carrier is assigned the same symbol based upon the bits output of the randomizer in Figure 31. [1]

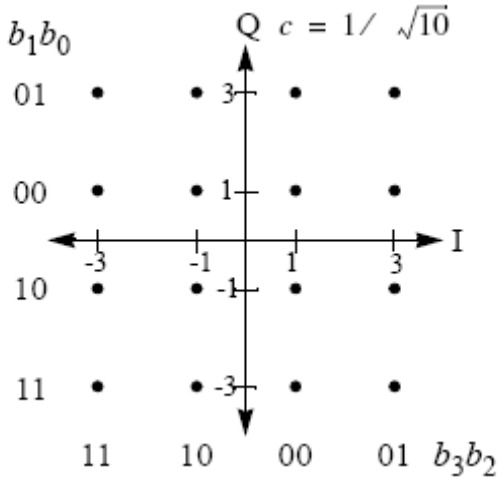

Figure 30. Gray Mapped 16–QAM (From Ref. [1].)

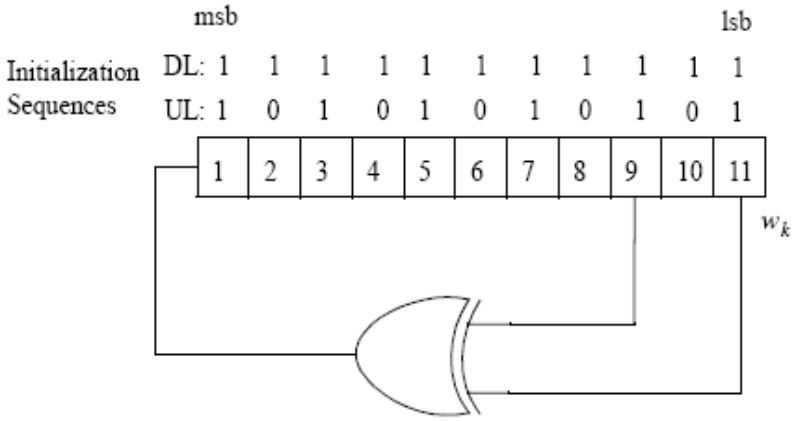

Figure 31. Pilot Symbol Generator (From Ref. [1].)

The magnitudes of the mapped symbols are then normalized according to the values in Table 7.

Modulation scheme	Normalization constant for unity average power
QPSK	$c = 1/\sqrt{2}$
16-QAM	$c = 1/\sqrt{10}$
64-QAM	$c = 1/\sqrt{42}$
256-QAM	$c = 1/\sqrt{170}$

Table 7. Normalized Power Constants (From Ref. [1].)

Pilot carriers are inserted, and the OFDM signal is converted into the time domain via the IFFT, which performs the IDFT function. The symbols are mapped onto the appropriate carriers as shown in Table 3. The CP is then attached to the symbol. To complete the DL subframe, the preamble and FCH are added to the data stream. [1]

Figures 32 and 33 show the resulting time domain and frequency domain, respectively, of a DL subframe with preamble. The frequency domain also shows the spectrum mask as prescribed in [1].

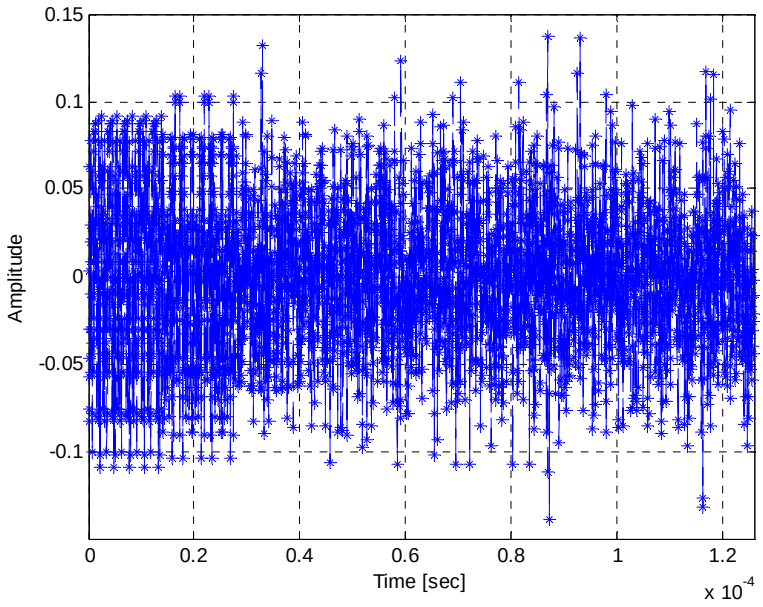

Figure 32. Transmitted Signal in the Time Domain

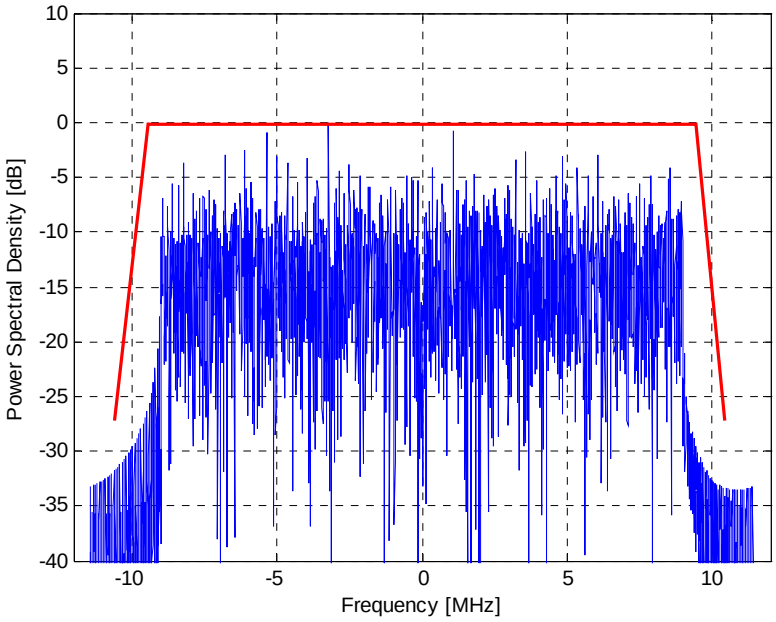

Figure 33. Signal with 20-MHz Bandwidth with Spectral Mask

C. RECEIVER

As stated earlier, any receiver is only as good as its synchronization. No system is able to successfully decode a signal if it cannot first accurately determine when and in

what spectrum the data was received, relative to where it was transmitted. OFDM requires special attention to the spectral state of the signal since it requires fine frequency synchronization in order to account for frequency offset and carrier phase rotation. In addition, it must be able to estimate the channel to use diversity and equalization.

After these various algorithms are employed in an effort to return the signal to its state before it was transmitted, the receiver then demodulates the signal using either hard decision or soft decision demodulation. Hard decision demodulation (HDD) simply outputs "1"s and "0"s based upon the magnitude relative to a given threshold. Soft decision demodulation (SDD) retains information about the reliability of the demodulation decision. The value of the bit has to do with its distance from the decision statistic threshold. Therefore, a larger value represents a more reliable decision. Coding gains are given later based on simulations with HDD and SDD. [6]

After the quantized bits are demodulated, they are de–interleaved. The operation that was done in the transmitter is reversed in order to place the bits in their proper order. The goal is for the burst errors to be sufficiently interspersed for the Viterbi decoder to correct. The bits are then de–punctured by adding dummy bits or erasures into the spots where the original sequence was punctured. A zero value of these bits should not affect the Viterbi algorithm. [1, 4]

The Viterbi algorithm is a ML codeword decoder [12]. It can use both HDD and SDD. In addition, SDD outputs can also be weighted to enhance the performance of the algorithm. The outputs are weighted by the squared channel amplitudes as follows [13]:

$$p_n = \left|\hat{H}_k\right|^2 \left|\hat{b}_n - b_n\right|^2, \tag{4.5}$$

where $\hat{H}_k$ is the channel amplitude of the k_{th} subcarrier, and $\left|\hat{b}_n - b_n\right|$ is the Euclidean distance with $\hat{b}_n$ as the SDD output and b_n as the threshold value. [13]

This weighting serves to reduce the effect of subcarriers that operate in a deep fade. Since the carrier is severely attenuated, its effect on the Viterbi decoder will correspondingly be attenuated. The effect can be seen later in Figure 43.

D. PERFORMANCE OF 802.16A IN AWGN

Table 6 showed the three available modulation schemes and their several code rates available to the BS on the DL. The modulation schemes which transmit more bits per symbol require higher SNR to function at reasonable bit error rates (BER). The rate 3/4 64–QAM, therefore, will require the highest SNR.

Figure 34 shows a 16–QAM and QPSK signal constellation using Matlab coding. The 16–QAM is in blue, and the QPSK is in green. The FCH is always transmitted using QPSK, and is the SIGNAL field [1]. Generally the decision boundaries are halfway between each constellation point. If the noise amplitude is large enough, the constellation points will cross the threshold resulting in an incorrect signal demodulation.

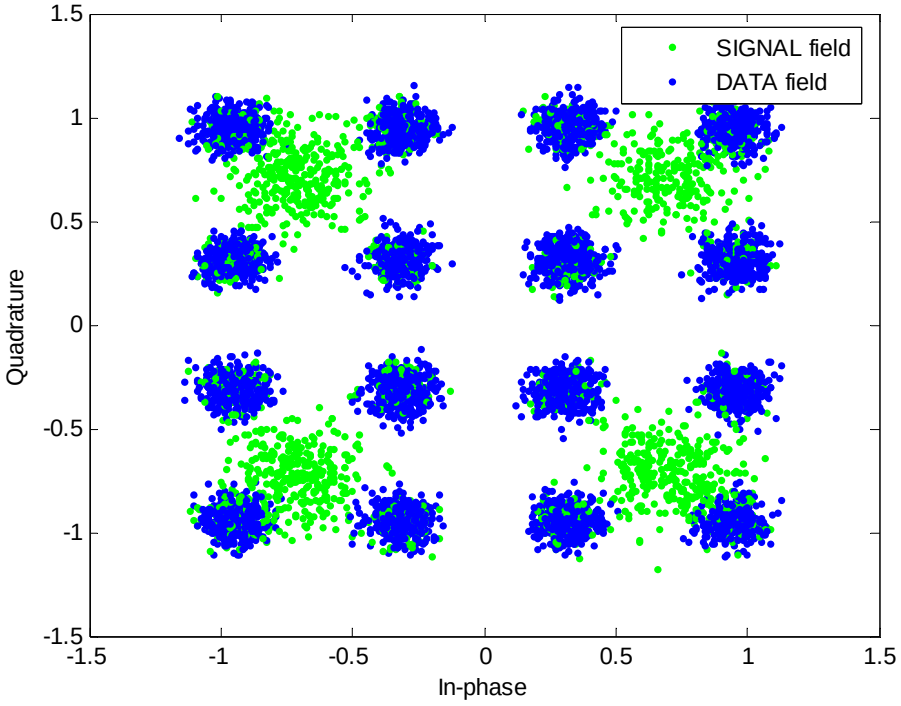

Figure 34. Rate 1/2 16–QAM Constellation in AWGN (SNR = 18 dB)

Hard–decision decoding and soft–decision decoding also produce different coding gains as shown in Figure 35. Since 802.16a is generally packet–oriented, a good metric is the packet error rate (PER), like in Figure 36. Each simulated packet was a DL subframe in the 802.16a standard. For r = 3/4 64–QAM, a coding gain of approximately 2.5 dB can be seen in Figure 35 between SDD and HDD. The raw theory curve represents a

coded signal at the input to the Viterbi decoder. The uncoded theory curve represents a signal without any FEC. Therefore, the uncoded theory has a coding gain over the raw theory equal to the inverse of the coding rate since the uncoded theory has more energy per symbol.

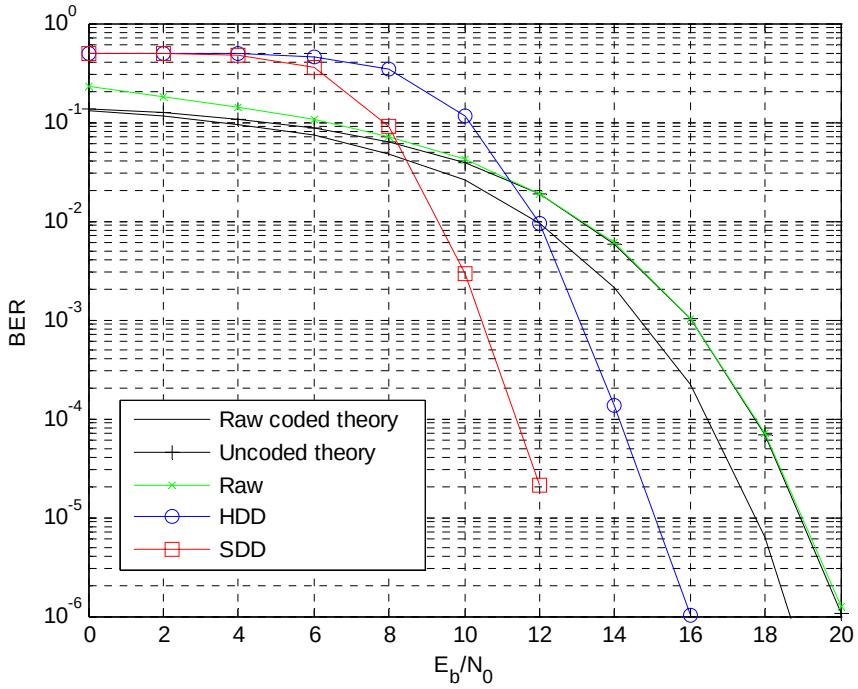

Figure 35. BER of Rate 3/4 64–QAM in AWGN

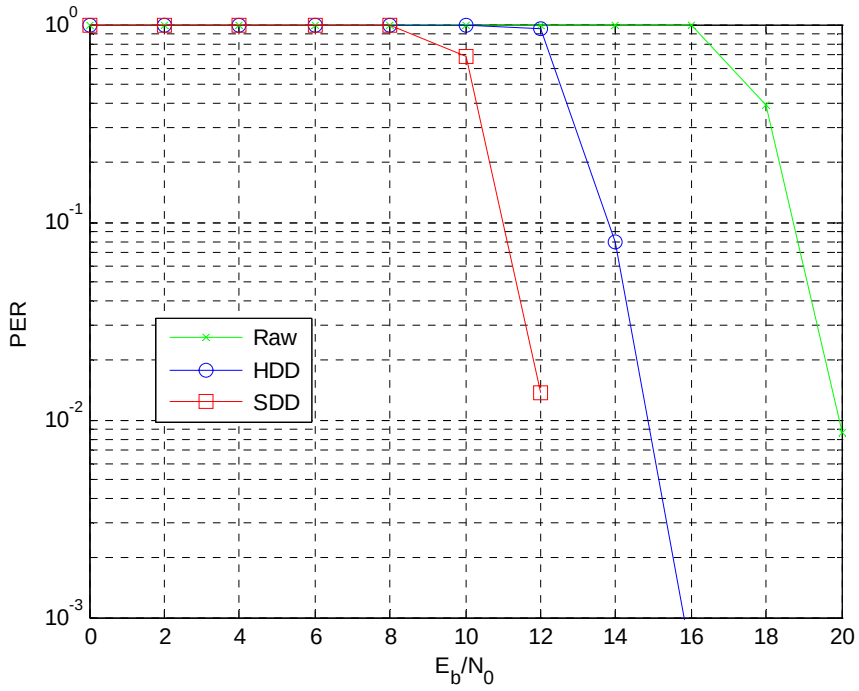

Figure 36. PER of Rate 3/4 64–QAM

For r = 2/3 64–QAM, the performance is slightly better, as seen in Figure 37, since r = 2/3 has a larger minimum distance than r = 3/4 and thus requires more distortion to cross a decision threshold. Therefore, the curves drop off a little more sharply and provide better performance. The PER shown in Figure 38, as in the r = 3/4 case, demonstrates the gain provided by both HDD and SDD. For r = 2/3, HDD provides a gain of 6 dB, while SDD provides a gain of 9 dB. In the HDD case, the coding gain improves by about 1 dB between r = 3/4 and r = 2/3. In both cases, the difference between HDD and SDD is 3 dB.

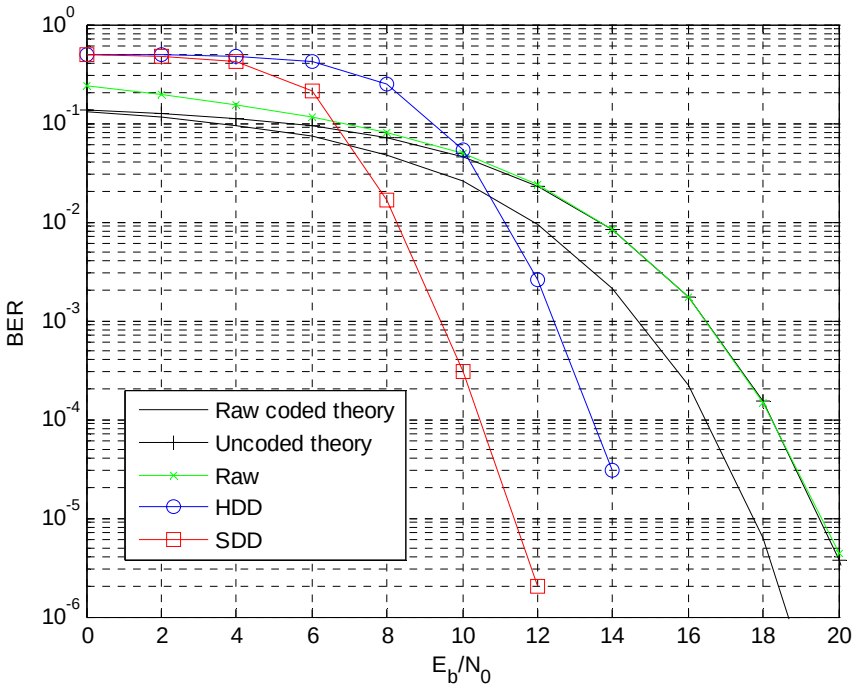

Figure 37. BER of Rate 2/3 64–QAM

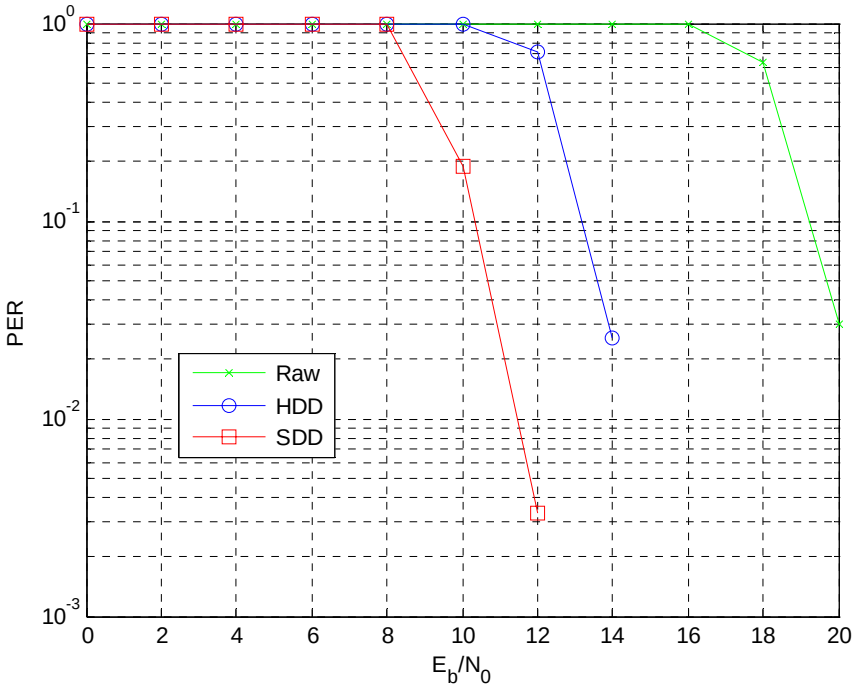

Figure 38. PER of Rate 2/3 64–QAM

The BER curves of all six available modulation schemes at the BS are provided in Figure 39. As is expected, the higher bit–per–symbol schemes require higher SNR for the same BER. In addition, the coding gain affects the BER of each modulation scheme, as seen above. With an SNR of 13 dB, each of the schemes passes 10^{-6} BER. The difference between r = 1/2 QPSK and r = 3/4 64–QAM is 8 dB.

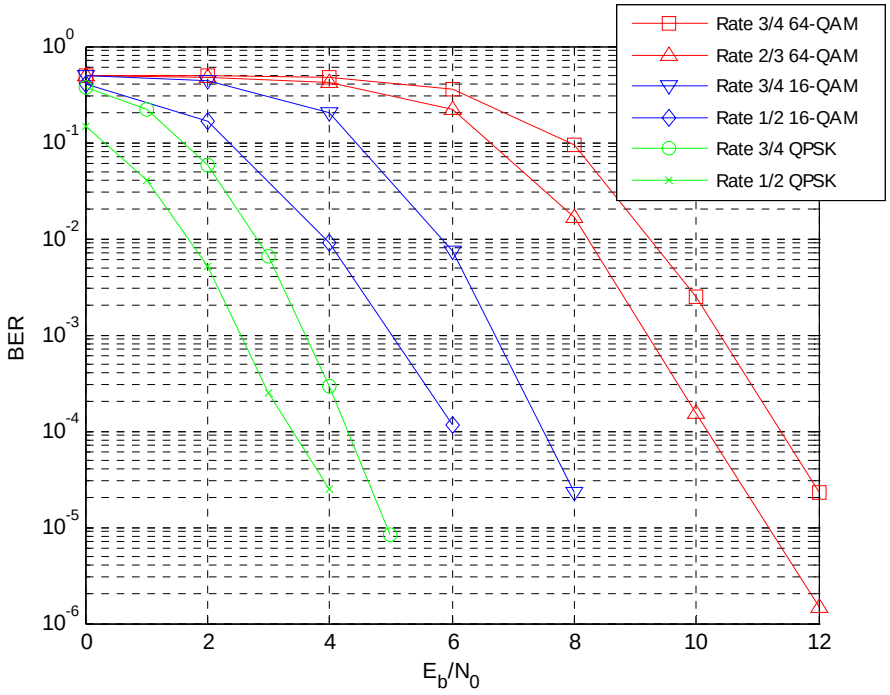

Figure 39. 802.16a BER in AWGN

In the PER case in Figure 40, different coding rates for QPSK did not provide any coding gain. Thus, the coding gain in BER only reduced the number of bit errors per packet.

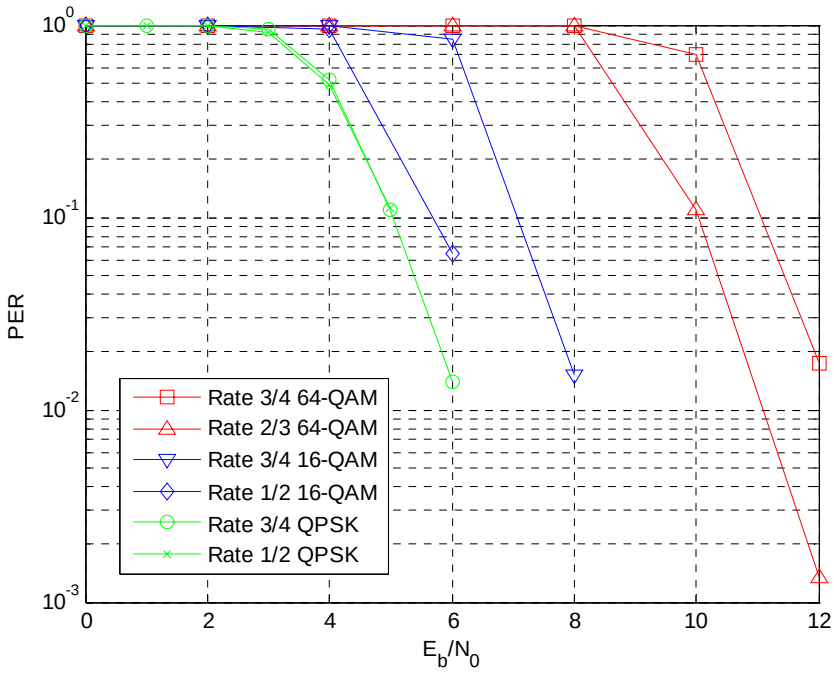

Figure 40. 802.16a PER in AWGN

Since the 802.16a standard often operates in an urban or suburban environment, the distances achievable by each rate and modulation scheme can provide a large cost difference in number of base stations and size of cells. Since the average path loss, $\overline{PL}(d)$ is dependent on distance according to [3]

$$\overline{PL}(d) \propto d^{n}, \tag{4.6}$$

where n is the path loss exponent. Some values of n are provided in [3]. The free space exponent is $n = 2$. Typical urban values vary between $n = 2.7$ and $n = 3.5$. If in an urban canyon, (no LOS due to height disparity in buildings) the path loss exponent can reach $n = 5$. In a mid–range urban environment $n = 3$, doubling the distance will create a path loss eight times as great, which is roughly 9 dB. In an urban canyon with $n = 5$, the same increase in path loss will be achieved by increasing the distance 1.5 times. Therefore, the range between $r = 1/2$ QPSK and $r = 3/4$ 64–QAM can vary from 1.5 to twice the distance. [3]

E. PERFORMANCE OF 802.16A IN MULTIPATH FADING

In a small–scale fading environment, the bit energy E_b is no longer a constant but becomes a random variable. For calculating probabilities, each subcarrier is assumed to be independently faded and thus a function of its own independent E_b. This practice can be optimistic since subcarrier spacing does not always exceed the channel's coherence bandwidth. This study used a Monte Carlo simulation with using a Matlab Graphical–User Interface (GUI). It was modified from the GUI used in [4] to simulate 802.11a. [6]

In order to determine the effects of fading, the simulations were run with perfect synchronization and channel estimation, both ideal cases. Typical RMS delay spread values in suburban or urban environments can range from 100 ns to 5300 ns. [5]

Figure 41 shows the signal constellation of a 16–QAM signal in a Rayleigh fading channel. Even at relatively low delay spread values, the signal is clearly distorted beyond possible demodulation. In order to get a usable signal out, the received signal must be equalized using an estimate of the channel derived from the preamble. Using equalization techniques written in Matlab codes, Figure 42 clearly shows the equalized 16–QAM signal. As a side effect, some of the noise samples are amplified. The performance can be further improved by multiplying the SDD outputs by the square of the channel amplitude as discussed above

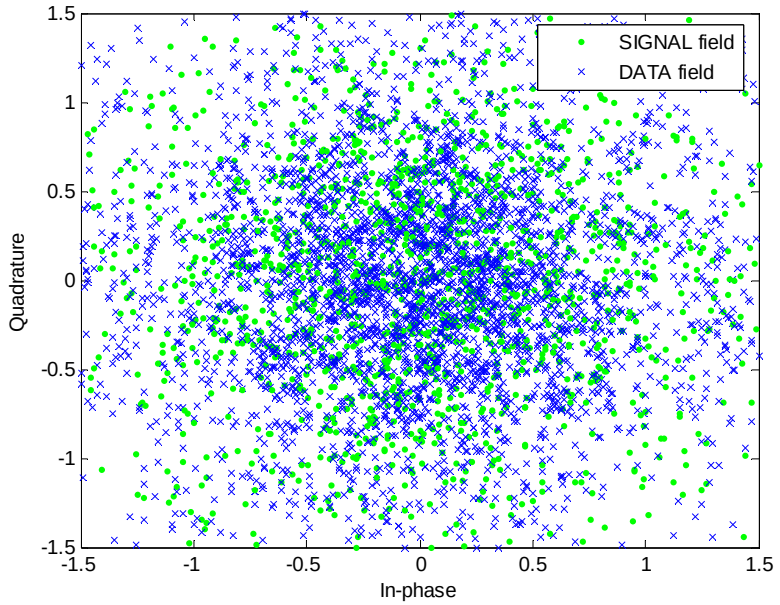

Figure 41. Signal Constellation in 50-ns RMS Delay Spread Rayleigh Fading Channel with SNR = 20 dB

.

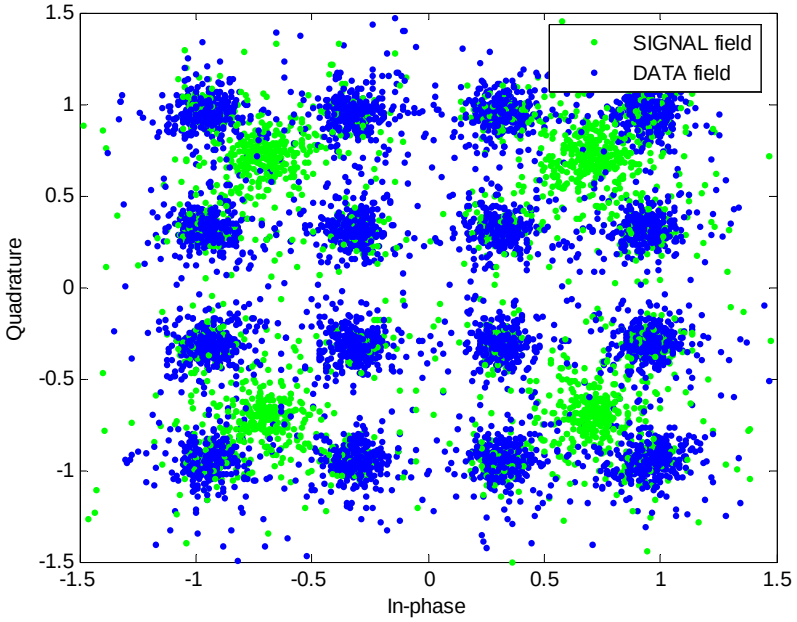

Figure 42. Equalized 16–QAM Signal in 50-ns RMS Delay Spread with SNR = 20 dB

The simulation of Figure 43 was run using r = 3/4 QPSK in a Rayleigh fading channel with RMS delay spread of 500 ns. This spread would represent a severe suburban or relatively benign urban environment.

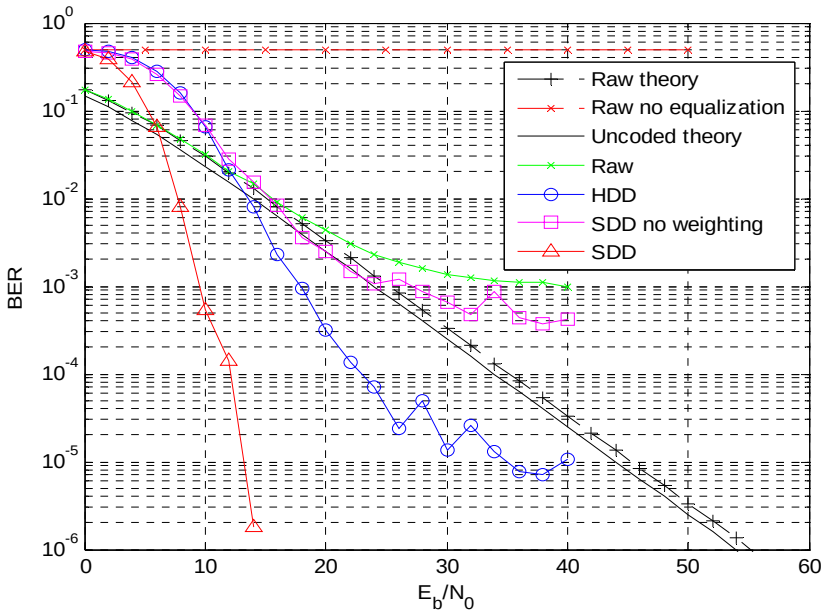

Figure 43. Rate 3/4 QPSK in RMS = 500 ns Delay Spread

As seen in Figure 43, the unequalized signal never provides usable data but hovers around a BER of 0.5. In this simulation, the HDD and un–weighted SDD cases both provide little or no coding gain since they hit a floor around $6x10^{-6}$ for unweighted SDD and $1x10^{-5}$ for HDD. The reason unweighted SDD performs more poorly than HDD is that the deeply faded subcarriers contribute the same amount to the SDD as the carriers which experience a relatively small amount of fading. Therefore, some of the noise is amplified. Weighted SDD, however, provides a coding gain of 39 dB and drops below 10^{-6}.

The coding gain between r = 1/2 and r = 3/4 for QPSK, seen in Figure 44, was around 6 dB at 10^{-6}. As in the AWGN case, the r = 3/4 code has a smaller Euclidean distance than the r = 1/2 code. The overall coding gain for the r = 1/2 code was 44 db, and it was 38 dB for r = 3/4 QPSK.

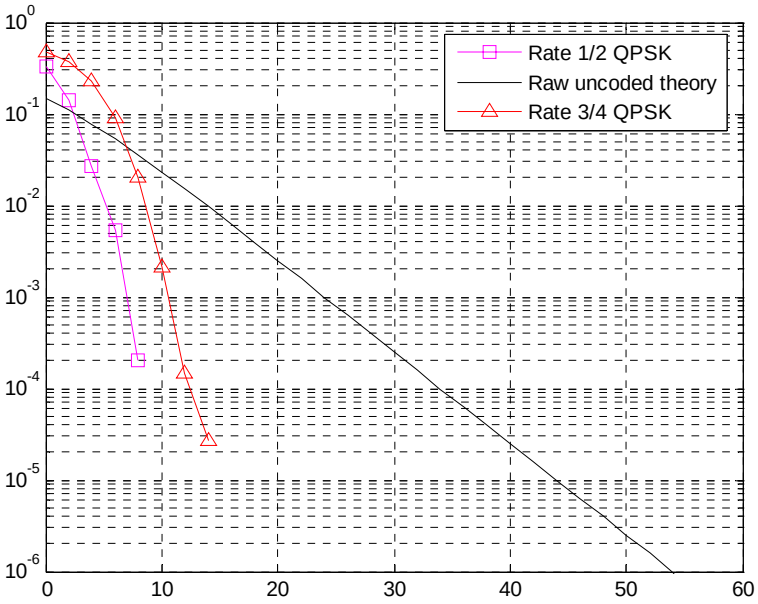

Figure 44. QPSK in a Rayleigh Fading Channel with RMS Delay Spread of 200 ns

Figure 45 shows the performance of 16–QAM in the same channel. The coding gain between rates is around 6 dB at the required BER, and the overall coding gain varies between 36 dB and 42 dB, which is 2 dB lower than for QPSK.

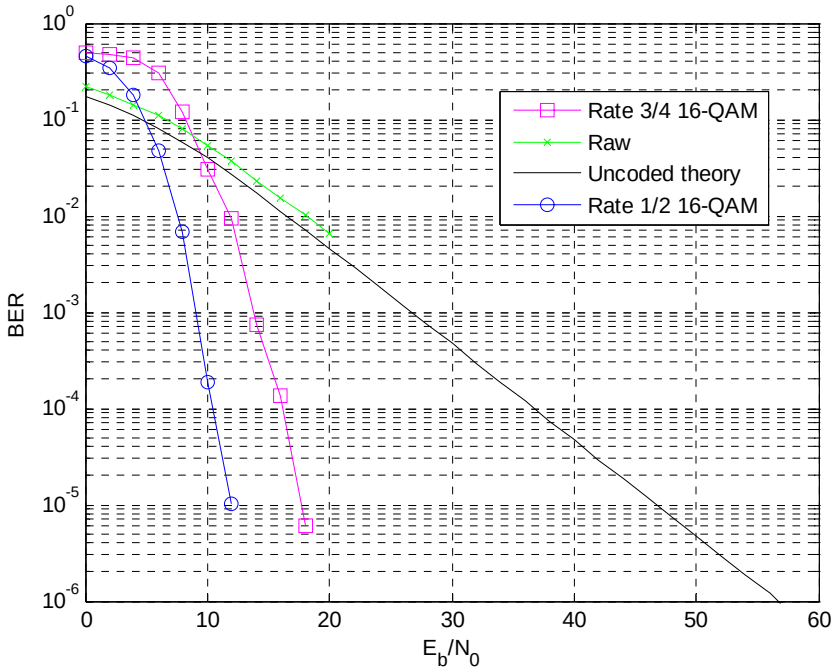

Figure 45. 16–QAM in 200-ns RMS Delay Spread Rayleigh-Fading Channel

Figure 46 for 64–QAM reveals a relative coding gain of roughly 3 dB. The difference is due to the fact that the coding change was different. For 64–QAM, the code changes between 2/3 and 3/4. The overall coding gain varies between 37 dB and 40 dB.

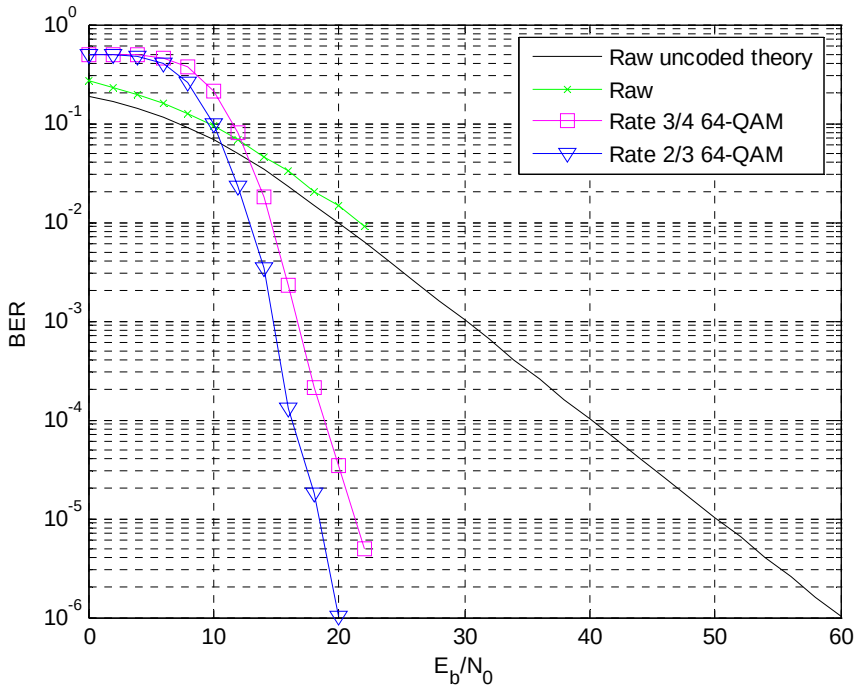

Figure 46. 64–QAM in RMS = 200 ns Rayleigh Fading Channel

F. SPACE–TIME CODING DIVERSITY

The IEEE 802.16a standard provides for the use of transmit diversity on the DL. The diversity scheme, known as Space–Time Coding (STC), uses both spatial and time diversity on the transmitter side. In any use of diversity, the effort is to decorrelate the multiple transmission or receptions in order to mitigate the detrimental effects of the channel. Since the L channels are independently fading, the probability that each channel will experience a deep fade at any particular frequency is p^L. [7] This type of transmission, or Multiple–Input Single–Output (MISO) diversity was originally proposed in [14].

Spatial or antenna diversity uses multiple antennas separated spatially to generate multiple independent channels. In 802.16a, STC uses two transmit antennas, as seen in Figure 47. In addition, each OFDM symbol is sent twice, possibility creating time diversity if the time between repeat of the symbols is longer than the coherence time.

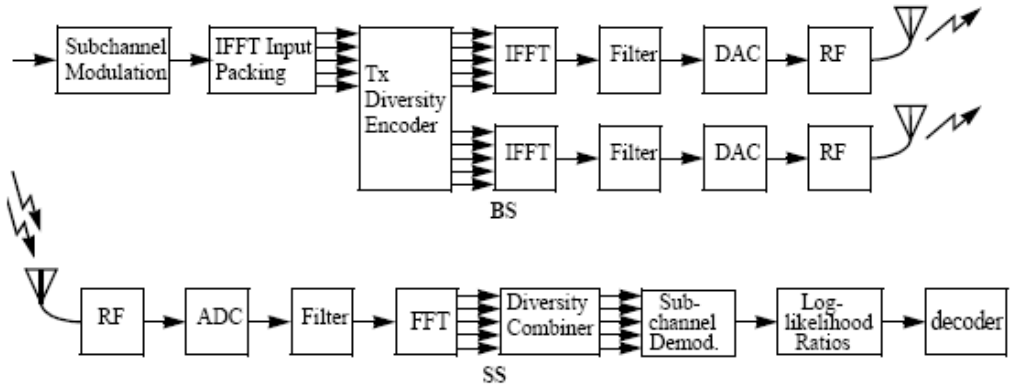

Figure 47. Block Diagram of STC Encoding and Decoding (From Ref. [1].)

In order to obtain a channel estimate, after the FCH is sent, antenna 1 transmits the short preamble. Thereafter, both antennas are used and thus STC is employed. Table 8 illustrates how each symbol is transmitted once from each antenna. Each received symbol with noise becomes [14]

$$\begin{aligned} r_0 &= r(t) = h_0 s_0 + h_1 s_1 + n_0 \\ r_1 &= r(t+T) = -h_0 s_1^* + h_1 s_0^* + n_1, \end{aligned} \tag{4.7}$$

where n_0 and n_1 are AWGN and h_0 and h_1 are the channel transfer functions given by [14]

$$\begin{aligned} h_0 &= \alpha_0 e^{j\theta_0} \\ h_1 &= \alpha_1 e^{j\theta_1}. \end{aligned} \tag{4.8}$$

	antenna 0	antenna 1
time *t*	s_0	s_1
time *t* + *T*	$-s_1^*$	s_0^*

Table 8. Space–Time Coding

The receiver combiner reconstructs the transmitted signals via the following equations: [14]

$$\begin{aligned} \hat{s}_0 &= h_0^* r_0 + h_1 r_1^* \\ \hat{s}_1 &= h_1^* r_0 - h_0 r_1^*. \end{aligned} \tag{4.9}$$

By substituting in the original transmitted signals, the received signals are seen to be scaled by the square of the magnitude of each channel as follows: [14]

$$\hat{s}_0 = (\alpha_0^2 + \alpha_1^2)s_0 + h_0^* n_0 + h_1 n_1^*$$
$$\hat{s}_1 = (\alpha_0^2 + \alpha_1^2)s_1 - h_0 n_1^* + h_1^* n_0. \quad (4.10)$$

Therefore, in order to normalize the reconstructed signals' amplitudes, they must be divided by the sum of the square of the channel amplitudes, similar to Maximal–Ratio Combining (MRC) receiver diversity.

STC transmit diversity also works well with popular receiver diversity techniques, including selection and MRC diversity [14]. In the instance of selection diversity, the above process is simply done for the receiver antenna with the strongest detected power. Since STC is similar to MRC, the technique naturally handles multiple receiver antennas. If the received signal matches its corresponding channel estimate (i.e., $r_0 \Leftrightarrow h_0$), then a Multiple–Input Multiple–Output system (MIMO) using STC and MRC with two receive antennas has the channel values of Table 9.

	rx antenna 0	rx antenna 1
tx antenna 0	h_0	h_2
tx antenna 1	h_1	h_3

Table 9. MIMO STC

The reconstructed signal is then [14]

$$\hat{s}_0 = h_0^* r_0 + h_1 r_1^* + h_2^* r_2 + h_3 r_3^*$$
$$\hat{s}_1 = h_1^* r_0 - h_0 r_1^* + h_3^* r_2 - h_2 r_3^*. \quad (4.11)$$

The simulation in Figure 48 was done in Matlab using a Rayleigh fading channel with RMS delay spread of 200 ns. STC was used on the transmit side, and Maximal–Ratio Combining (MRC) as simulated in [4] was used on the receive side. The parameter *L* denotes the number of antennas used. When STC was used, two transmit antennas were used, and the rest were on the receiver. When STC was not used, all the antennas were at the receiver. The raw Rayleigh faded and AWGN outputs are provided to show coding gain.

In the case without diversity, the BER duplicates that in Figure 46. The coding gain is roughly 37 dB, since the raw output cross 10^{-6} at an SNR of 60 dB. As can be

seen, STC performs slightly more poorly than MRC using only two transmit or two receive antennas. However, in the case of two transmit and two receive antennas using STC, or four receive antennas using MRC, the performance is nearly the same. In each use of diversity, the performance exceeded that of raw AWGN, meaning that the channel effects were corrected. In addition, a coding gain was seen over SDD–coded r = 3/4 64–QAM in a purely AWGN channel. Therefore, diversity reduces the effects even of noise at the receiver.

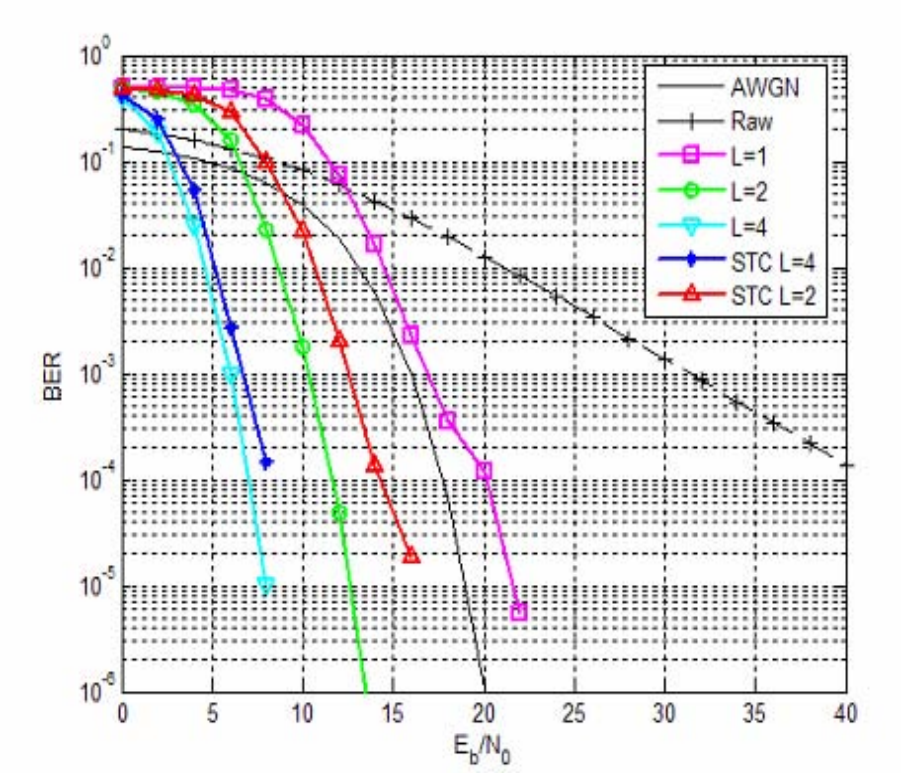

Figure 48. Rate 3/4 64–QAM using Maximal–Ratio Combining Receiver Diversity and STC Transmit Diversity

G. SUMMARY

This chapter has provided an overview of the transmit and receive processes in the 802.16a system. It then provided simulated outputs in only AWGN and in several channels indicative of outdoor fading environments. The graphs provided data on the effects of fading since the other synchronization factors were assumed to be ideal.

In AWGN, a gain of 8 dB was seen between the highest and lowest performing modulation scheme, which translated to a distance difference between 1.5 and 2 times,

depending upon the environment. In addition, the differing coding rates provided different coding gains as expected. In a fading environment even the strongest signals will experience severe distortion preventing successful decoding. Therefore, equalization is necessary in order to have an operable system.

Diversity proved its impact in mitigating the effects of a fading channel. Through interleaving and frequency diversity and STC and MRC and spatial and time diversity, the effects of a fading channel corrected. Also, the performance can even exceed that of pure AWGN using diversity. Therefore, even the highest data rate can provide reliable data in as little as 9–10 dB.

The next chapter deals with some of the conclusions that can be drawn from the simulations and further work that can be done to analyze the 802.16a standard.

THIS PAGE INTENTIONALLY LEFT BLANK

V. CONCLUSIONS AND FUTURE WORK

Broadband Wireless Access is an emerging internet technology that is beginning its market penetration. As an answer to lower–infrastructure broadband internet, the 802.16a standard has many provisions that make the high data rates possible even in severely–faded cases. The system is possible using OFDM in order to transmit higher bit rates in a spectrally efficient manner. In addition, the standard incorporates other elements of current research and technology including adaptive antenna systems (AAS) and STC. Both promise to provide higher link margins and extra coding gain in any fading environment. The standard also provides the means for users away from major population centers to receive broadband internet without having to use satellite systems.

A Matlab simulation toolbox and analysis of synchronization and performance were developed by the author for the 802.16a standard. Modified from the 802.11a standard, the toolbox can be modified for any OFDM system and provides indicative results of the direction of most OFDM systems.

A. CONCLUSIONS

Chapter II provided an overview of multipath fading and the 802.16a physical layer. In order to account for a worst–case scenario, a Rayleigh fading channel model was chosen, which simulates non–LOS communication. An overview of each of the three operating methods in 802.16a was also provided. The focus of this study was the OFDM mode.

Chapter III modified the work of [4] and applied it to 802.16a. The synchronization algorithm was able to successfully detect the packet and perform frame and frequency synchronization within acceptable limits. In addition, the methods of carrier phase tracking, channel estimation, and equalization were covered.

Chapter IV provided performance analysis of the 802.16a standard in AWGN and multipath fading as well as employing diversity. The coding gains provided by HDD and SDD were shown. The effect of equalization and weighted SDD on a fading channel was also shown. Both are necessary especially at higher RMS delay spreads, which will be

more indicative of the types of environments in which 802.16a will be operating. Finally, the effect of diversity was seen. Combining STC and MRC to create a MIMO system, the fading effect of the channel was corrected and the performance without diversity in AWGN was exceeded. The use of diversity promises to greatly enhance performance and capacity.

B. FUTURE WORK

This study only provided an initial look at 802.16a. As an emerging technology, which is itself using various other technologies, there is opportunity for much more study on the standard. The 802.16a standard comes with many different features, which can be capitalized upon to further improve throughput. A few of these that were not simulated in this study are the Reed–Solomon convolutional concatenated code and Advanced Antenna System (AAS). In addition, the capacity and performance of the OFDMA mode can be analyzed.

Also, the techniques used in this study and [4] to synchronize with an 802.16a signal can be applied to an 802.16a system to attempt to synchronize with and decode an actual signal.

LIST OF REFERENCES

[1] IEEE 802.16a–2003, "Air Interface for Fixed Broadband Wireless Access Systems—Amendment 2: Medium Access Control Modifications and Additional Physical Layer Specifications for 2-11 GHz," IEEE Std 802.16a-2003. http://standards.ieee.org/getieee802/download/802.16a-2003.pdf (last access June 2005.)

[2] T. Cooklev, *IEEE Wireless Communication Standards: A Study of 802.11, 802.15, and 802.16*, IEEE Press, 2004.

[3] T.S. Rappaport, *Wireless Communications: Principles and Practice*, 2nd ed., Prentice Hall, Upper Saddle River, NJ, 2002.

[4] M. Sekgos, "Advanced Techniques to Improve the Performance of OFDM Wireless LAN," Master's Thesis, Naval Postgraduate School, Monterey, CA, June 2004.

[5] IEEE 802.16 Broadband Wireless Access Working Group, "Channel Models for Fixed Wireless Applications," July 2001. http://grouper.ieee.org/groups/802/16/tg3/contrib/802163c-01_29r4.pdf (last accessed June 2005.)

[6] B. Sklar, *Digital Communications: Fundamental and Applications*, 2nd ed., Prentice Hall, Upper Saddle River, NJ, 2001.

[7] P. Z. Peebles, Jr., *Probability, Random Variables, and Random Signal Principles*, 4th ed., McGraw Hill, New York, 2001.

[8] T. M. Schmidl and D. C. Cox, "Low–Overhead, Low–Complexity [Burst] Synchronization for OFDM," *IEEE International Conference on Communications*, Vol. 3, pp 1301–1306, 1996.

[9] T. Pollet, M. van Bladel, and M. Moeneclaey, "BER Sensitivity of OFDM Systems to Carrier Frequency Offset and Wiener Phase Noise," *IEEE Trans. on Communications*, Vol. 43, Issue 2, Part 3, pp. 191–193, February, March, April 1995.

[10] P. H. Moose, "A Technique for Orthogonal Frequency Division Multiplexing Frequency Offset Correction," *IEEE Trans. on Communications*, Vol. 42, No. 10, pp. 2908–2914, October 1994.

[11] X. Wang and H. V. Poor, *Wireless Communication Systems: Advanced Techniques for Signal Reception*, Prentice Hall, Upper Saddle River, NJ, 2004.

[12] L. H. Lee, *Error–Control Convolutional Coding*, Artech House, Boston, 1997.

[13] J. G. Proakis, *Digital Communications*, 4th ed,. McGraw Hill, New York, 2001.

[14] S. M. Alamouti, "A Simple Transmit Diversity Technique for Wireless Communications," *IEEE Journal on Select Areas of Communications*, Vol. 16, No. 8, pp. 1451-1458, October 1998.

INITIAL DISTRIBUTION LIST

1. Defense Technical Information Center
   Ft. Belvoir, Virginia

2. Dudley Knox Library
   Naval Postgraduate School
   Monterey, California

3. Chairman, Department of Electrical and Computer Engineering, Code EC
   Naval Postgraduate School
   Monterey, California

4. Professor Tri T. Ha, Code EC/Ha
   Department of Electrical and Computer Engineering
   Naval Postgraduate School
   Monterey, California

5. Professor David Jenn, Code EC/Jn
   Department of Electrical and Computer Engineering
   Naval Postgraduate School
   Monterey, California

5. Jared Allen
   Concord, California